Information Fusion 68 (2021) 67–84

Contents lists available at ScienceDirect

Information Fusion

journal homepage: www.elsevier.com/locate/inffus

# 40 years of sensor fusion for orientation tracking via magnetic and inertial measurement units: Methods, lessons learned, and future challenges

Milad Nazarahari, Hossein Rouhani *

*Department of Mechanical Engineering, University of Alberta, Donadeo Innovation Centre for Engineering, Edmonton, Alberta T6G 1H9, Canada*

ARTICLE INFO

*Keywords:*
Sensor fusion algorithm
Attitude and heading reference system
Linear/extended Kalman filter
Complementary Filter
Adaptive gain tuning
Magnetic and inertial measurement unit

ABSTRACT

Technological developments over the past two decades have resulted in the development of more accurate and lightweight low-cost magnetic and inertial measurement units (MIMUs). These developments have allowed the extensive application of MIMUs in various fields, specifically tracking the 3D orientation of a rigid body. Despite recent technological improvements, measurements from a tri-axial gyroscope, accelerometer, and/or magnetometer inside the MIMU are characterized by uncertainties. Numerous studies have been conducted to address these uncertainties and develop sensor fusion algorithms (SFAs) to estimate the 3D orientation accurately and robustly. This paper contributes to these efforts by providing a survey of the state-of-the-art SFAs for orientation estimation. We surveyed +250 publications, categorized the SFAs with various structures, identified the modifications proposed to improve their performance, and discussed the strengths and weaknesses of these approaches. We found that, while early SFAs were mostly a vector observation algorithm or an extended Kalman filter, to improve the computational efficiency, more recent works have developed SFAs with a complementary filter or complementary Kalman filter structure. At the same time, to improve the performance of the SFAs, several research teams have proposed various modifications to the basic structure of these filters, such as adaptive gain tuning or imperfect measurement rejection. We also provided an outlook on the lessons learned as well as the main challenges related to SFAs and discussed the practical steps toward developing an effective SFA. We have identified the need for benchmarking studies as the main challenge at the moment. This paper is among the first surveys which provide such breadth of coverage across different SFAs for tracking orientation with MIMUs.

## 1. Introduction

Magnetic and inertial measurement units (MIMUs), comprised of a tri-axial accelerometer, gyroscope, and magnetometer, are used to track the displacement and orientation of a rigid body in real-time. Because of their lightweight, small size, and long battery life [1,2], MIMUs have been used extensively as an ideal tool in aerospace, unmanned vehicle navigation, robotics, and human motion tracking. However, in almost all applications, whether the 3D joint angle measurement in an ambulatory human motion tracking system [3] or displacement estimation in a dead-reckoning system [4], the MIMU orientation must be first calculated using a sensor fusion algorithm (SFA), also known as attitude and heading reference system (AHRS).

Raw MIMU data can be used to estimate orientation under specific conditions. In particular, the MIMU's accelerometer measures the gravitational acceleration and can be used to compute the attitude. Also, in a magnetically neutral environment, the magnetometer measures the geomagnetic field, which can be used to estimate the yaw angle. Furthermore, the gyroscope measures the angular velocity (rate of change of orientation), which can be used to calculate the change in orientation using numerical strap-down integration (SDI).

However, using the accelerometer, gyroscope, and magnetometer alone may yield poor estimations in terms of accuracy or robustness due to various sources of error [5]. For example, accelerometers are not suitable for orientation estimation during dynamic tasks as they measure the external non-gravitational acceleration (due to motion) in addition to the gravitational acceleration. Also, the geomagnetic field could be distorted by the presence of ferrous materials, specifically during indoor motion tracking, which makes magnetometer-based estimations inaccurate. Moreover, because the cumulative error of the SDI increases unbounded over time, MEMS gyroscopes are not suitable for orientation

* Corresponding author at: Department of Mechanical Engineering, University of Alberta, 10-368 Donadeo Innovation Centre for Engineering, 9211-116 Street NW, Edmonton, ABT6G 1H9, Canada.

*E-mail addresses:* nazaraha@ualberta.ca (M. Nazarahari), hrouhani@ualberta.ca (H. Rouhani).

https://doi.org/10.1016/j.inffus.2020.10.018
Received 5 August 2020; Received in revised form 25 September 2020; Accepted 29 October 2020
Available online 2 November 2020
1566-2535/

**Nomenclature**

| | |
|---|---|
| AHRS | Attitude and heading reference system. |
| DCM | Direction cosine matrix. |
| FQA | Factored quaternion algorithm. |
| GDA | Gradient descent algorithm. |
| GNA | Gauss-Newton algorithm. |
| L/E/CKF | Linear/extended/complementary Kalman filter. |
| L/NCF | Linear/non-linear complementary filter. |
| MIMU | Magnetic and inertial measurement unit. |
| PSO | Particle swarm optimization. |
| QUEST | QUaternion ESTimator. |
| SDI | Numerical strap-down integration. |
| SFA | Sensor fusion algorithm. |
| TRIAD | TRi-axial attitude determination. |
| VO | Vector observation. |
| w.r.t. | With respect to |

estimation during long-duration tasks. Thus, various SFAs have been proposed in the literature to achieve an accurate and reliable estimation.

### 1.1. *Orientation parametrization*

Rigid body orientation can be expressed via one of the following parametrizations: (i) Euler angles, i.e., roll and pitch (also known as the attitude) and yaw (also known as the heading); (ii) quaternions; or (iii) direction cosine matrix (DCM) [6,7]. Euler angles can be used when an intuitive physical meaning of the estimated orientation is needed. For example, in controlling an unmanned vehicle [8], measuring human joint angles, or tracking in an augmented reality device [9]. However, under certain configurations, there are singularities associated with this parametrization that make Euler angles unsuitable for most control or tracking applications.

Quaternion or DCM parametrization could be used to express/calculate the orientation without singularity in a computationally-efficient manner [10,11]. However, the unconstrained estimation of these parametrizations would lead to an ambiguous and meaningless representation. In particular, a *quaternion parametrization of orientation* is an element of the quaternion group, i.e., homeomorphic to rotation group $SO(3)$, with $S^3$ as its domain [12]. Therefore, to reduce its degrees of freedom from four to three, consistent with the dimension of the $SO(3)$, a constrained quaternion estimation is required, such as enforcing the unit norm constraint after estimation. See more on constrained estimation in [12,13]. A similar hard constraint must be used when using DCM parametrization [14,15].

### 1.2. *Previous surveys on SFAs*

Previous surveys have reviewed the literature related to MIMUs with a focus on applications [16–21], technical developments [4,17,22,23], and/or experimental comparison. However, in line with the aim of the present paper, in this section, we review the previous surveys of SFAs for MIMU orientation estimation only. Table 1 summarizes the surveys with a focus on the experimental comparison. Table 1 identifies the filter with the best performance in each survey and provides the details of the SFAs tested, parameter tuning strategies, and experimental validations.

Cavallo et al. [24] compared the estimation accuracy of three SFAs, their proposed Extended Kalman Filter (EKF) and SFAs in [25,26], using a MIMU mounted on KUKA Youbot robot while the accelerometer and magnetometer were calibrated using a 3D-ellipsoid fitting method [27]. The robot measured the reference (true) orientation during slow (18 deg/s) and fast (45 deg/s) trajectory tracking motions. Filippeschi et al. [10] performed an experimental study to compare five SFAs [28–32] for

**Table 1**
Review of the previous literature surveys of the sensor fusion algorithms, including the tested algorithms, the gain selection procedure, the used reference system for validation, the type experiments, and the algorithm(s) concluded to have the best performance. Abbreviations used in the table are described in the table footnotes.

| Study | Sensor Fusion Algorithms | Filter Parameters | Reference | Experiments (duration in seconds) | Selected Filter |
|---|---|---|---|---|---|
| [24] | PEKF, [25,26] | EC | Robot [182] | Slow & fast motions of robotic arm (≤45s) | PEKF |
| [10] | [28–32] | EC | MCS | Elbow, forearm & shoulder functional tasks (≤15s) | Acc.: [28] Corr.: [31] |
| [33] | [29,34–36] | EC | MCS | Random motions (≤20), Treadmill walking (≤30s) | [36] |
| [37] | PEKF, KF | EC | MCS | Random head motions (≤35s) | PEKF |
| [38] | [25,39–41] | EC | MCS | Static and dynamic tests in magnetically clean & disturbed environments (≤60s) | [41] |
| [42] | SDI, [25,37] | EC | MCS | Daily routine tasks (≤60s), Walking (≤180s) | [37] |
| [183] | [25,184] | EC | None | Single axis rotations (≤250s) | [184] |
| [39] | [122,129] | EC | MCS | Daily routine tasks (≤60s), Walking (≤180s) | [129] |
| [43] | [25,37,44], XKF | OP | MCS | Slow, medium & fast random rotations (≤70s) | Slow/medium: XKF, Fast: [37] |
| [185] | [25,26,143] | OP | MCS | Quadcopter motion adopted from [186] | [26] |
| [45] | [25,26,46–49] | EC | MCS | Smartphone data during various activities (≤180s) | [49] |
| [187] | [25,26] | EC | MCS | Various walking tests, adopted from [188] | [25] |
| [189] | [25,26,80,190] | OP | Synthetic | - | [25,26] |
| [191] | [192], modified [127] | EC | MCS | Material handling task (≤60s) | Modified [127] |

**- Sensor Fusion Algorithms:** PEKF: Proposed Extended Kalman Filter by the study; XKF: Xesne proprietary Kalman Filter; SDI: Strap-down integration.
**- Filter Parameters:** EC: Selecting the sensor fusion algorithm's gain(s) by trial-and-error; OP: Selecting the sensor fusion algorithm's gain(s) by a rigorous search.
**- Reference:** MCS: Gold-standard camera motion-capture system. Synthetic: used synthetic MIMU data.
**- Selected Filter:** Acc: Selected based on accuracy; Corr: Selected based on correlation.

wrist position tracking. They used orientation and length of the trunk, upper arm and forearm were used to estimate the wrist position. However, the accuracy of the SFAs was not directly comparable for the following reasons: (i) one method required visual reference for position tracking; (ii) methods were different in terms of constraints of the kinematic chain; and (iii) parameters of the methods were not selected systematically.

Young [33] compared the EKF proposed in [29] with different Complementary Filters (CFs) presented in [34–36]. After calibrating sensors for offset and scale errors, the accuracy of the SFAs was evaluated during gentle random motions and over treadmill walking at a normal pace. They concluded that in general, CFs with lower computational complexity could outperform KFs for human motion tracking, as CFs have no assumption about the process dynamics. Also, they showed that because of the lower computational complexity and minimal loss of accuracy, the use of non-optimal vector observation (VO) algorithms, such as TRi-axial Attitude Determination (TRIAD), is preferred compared to optimal ones, such as the QUaternion ESTimator (QUEST). More recently, Sabitini [37] provided a general survey of SFAs, including algorithms based on VOs and KFs, with great emphasis on practical aspects such as SFA gain selection.

Fan et al. [38] performed a systematic review of standard strategies for reducing the effect of magnetic disturbance on the accuracy and robustness of SFAs. They also compared the accuracy of five SFAs, [25, 39–41], and concluded that a "good" filter must have the following three features: (i) gyroscope drift compensation; (ii) decoupling attitude from yaw estimation; and (iii) an adaptive strategy to reject magnetic distortions. Similarly, Ligorio and Sabatini [39] reviewed the main magnetic disturbance compensation strategies used in KFs and showed that model-based approaches (estimating the magnetic disturbance at each iteration using a stochastic model) had the best performance.

Bergamini et al. [42] used routine manual tasks such as teeth/hair brushing and walking along a ∞-shaped pathway to compare the accuracy of SDI with the CF proposed by Madgwick et al. [25]and the KF proposed by Sabatini [37]. This study showed that the tested CF and KF were significantly more accurate than SDI for yaw estimation and that the two SFAs achieved similar accuracy. Using the optimal SFAs gains, Caruso et al. [43] analyzed the performance of four SFAs ([25,37,44], and Xesne proprietary KF) and concluded that the performance of SFAs depends on the experimental conditions, such as the rate of rotations during experiments. Michel et al. [45] compared the accuracy and robustness of six SFAs ([25,26,46–49]) using smartphone data during a variety of daily routine activities. They showed that the overall performance of the nonlinear CF proposed by Martin and Salaun [49] was best, but SFAs with a simpler structure and lower computational complexity, such as [25] and [26], could be highly beneficial for saving the battery life of the smartphone. See [50] for a more detailed study on the energy characterization of CF and KF.

However, the mentioned works only surveyed a limited number of SFAs, i.e., in total, 30 filters were tested in the abovementioned works, and only 4 of them were used in more than two studies. Therefore, in this paper, we reviewed a wide range of SFAs for orientation tracking with MIMUs, including VOs, CFs, Linear KFs (LKFs), EKFs, and Complementary KFs (CKFs). We did not, however, review fusing strategies such as the Unscented KF, Cubature KF, and Particle filter, or the use of other technologies for orientation tracking, whether alone or together with MIMUs. In summary, this review sought to answer the following question: how can MIMU signals be fused for orientation tracking? To answer this question, we provided a survey on state-of-the-art strategies, including SFAs based on VO, CF, and LKF/EKF/CKF families.

## 2. Literature survey

### 2.1. MIMU model

In this section, we present the MIMU model commonly used in developing SFAs [51,52]. Gyroscope readout, $y_G$, can be modelled as the summation of the true angular velocity, $\omega$, the bias $b_G$, and a white noise term, $\mathfrak{v}_G$, as in (1a),

$$y_{G,\,k} = K_G \omega_k + b_{G,k} + \mathfrak{v}_{G,\,k} \tag{1a}$$

$$b_{G,k} = b_{G,k-1} + \mathfrak{w}_{b,\,k} \tag{1b}$$

where $K_G$ is the scale factor matrix, and (1b) models $b_G$ as a first-order Markov process driven by white Gaussian noise, $\mathfrak{w}_b$. Accelerometer readout, $y_A$, can be modelled as the summation of the external non-gravitational acceleration, $\mathfrak{a}$, the gravitational acceleration, $g$, the bias $b_A$, and a white noise term, $\mathfrak{v}_A$, as in (2a),

$$y_{A,\,k} = K_A[\mathfrak{a}_k + g_k] + b_{A,k} + \mathfrak{v}_{A,\,k} \tag{2a}$$

$$\mathfrak{a}_k = c_a \mathfrak{a}_{k-1} + \mathfrak{w}_{\mathfrak{a},\,k} \tag{2b}$$

where $K_A$ is the scale factor matrix, and (1b) models $\mathfrak{a}$ as a first-order low-pass filtered ( $0 \le c_\mathfrak{a} < 1$ is the cut-off frequency of the filter) white Gaussian noise process. The bias term $b_A$ was commonly obtained through a calibration procedure [27,53] or estimated during orientation tracking as part of the KF state vector [54,55]. Finally, the magnetometer readout, $y_M$, can be modelled as the summation of the true geomagnetic field, $m$, magnetic distortion, $\mathfrak{d}$, and a white noise term, $\mathfrak{v}_M$, as in (3a),

$$y_{M,\,k} = K_M m_k + \mathfrak{d}_k + \mathfrak{v}_{M,\,k} \tag{3a}$$

$$\mathfrak{d}_k = c_d \mathfrak{d}_{k-1} + \mathfrak{w}_{\mathfrak{d},\,k} \tag{3b}$$

where $K_M$ is the scale factor matrix, and (3b) models $\mathfrak{d}$ as a first-order low-pass filtered ( $0 \le c_\mathfrak{d} < 1$ is the cut-off frequency of the filter) white Gaussian noise process.

### 2.2. Strap-down integration (SDI)

While SDI is not an SFA on its own, we dedicate a separate section to it as it is the core of almost all CFs and KFs. The numerical SDI of gyroscope readout, $y_G$, can be used to update the orientation with respect to (w.r.t.) a known orientation as in (4a) [56],

$$\begin{cases} q_{k+1} = \exp\left(\Omega\left(y_{G,\,k}\right)T_s\right)q_k \\ \quad q_0 = q(0) \end{cases} \tag{4a}$$

$$\Omega(y_G) = \frac{1}{2}\begin{bmatrix} 0 & -y_{G,x} & -y_{G,y} & -y_{G,z} \\ y_{G,x} & 0 & y_{G,z} & -y_{G,y} \\ y_{G,y} & -y_{G,z} & 0 & y_{G,x} \\ y_{G,z} & y_{G,y} & -y_{G,x} & 0 \end{bmatrix} \tag{4b}$$

where $q$ is the quaternion parametrization of orientation, $\Omega(y_G)$ is a 4× 4 skew-symmetric matrix shown in (4b), $\exp(\cdot)$ is the matrix exponential operator, which can be estimated using the Taylor series or Padé approximation, $T_s$ is the sampling period of the MIMU, and $q(0)$ is the known initial orientation. Lee and Choi [57] showed that when using the Taylor series to calculate $\exp(\cdot)$, the approximation order highly depends on (i) the sampling rate of the MIMU and (ii) the magnitude of the $y_G$. Equation (4a) can also be extended to account for the relative angular velocity of (i) the Earth's frame w.r.t. the inertial frame and (ii) the navigation frame w.r.t. the Earth's frame [58].

Nevertheless, SDI has two disadvantages: (i) the initial orientation must be known; and (ii) the gyroscope bias, $b_G$, results in an increasing cumulative error in the estimated orientation due to the numerical integration (see [59] for comparison of the drifts obtained from the SDI and a KF). To address the former, $y_A$ and $y_M$, along with a VO algorithm (described in Section 2.3), can be used to calculate $q(0)$. To address the latter, various SFAs have been developed to use $y_A$ and/or $y_M$ to correct the SDI drift over time. Also, using SFAs, $b_G$ can be estimated at each time instant based on a stochastic model, as in (1b), to correct the $y_G$

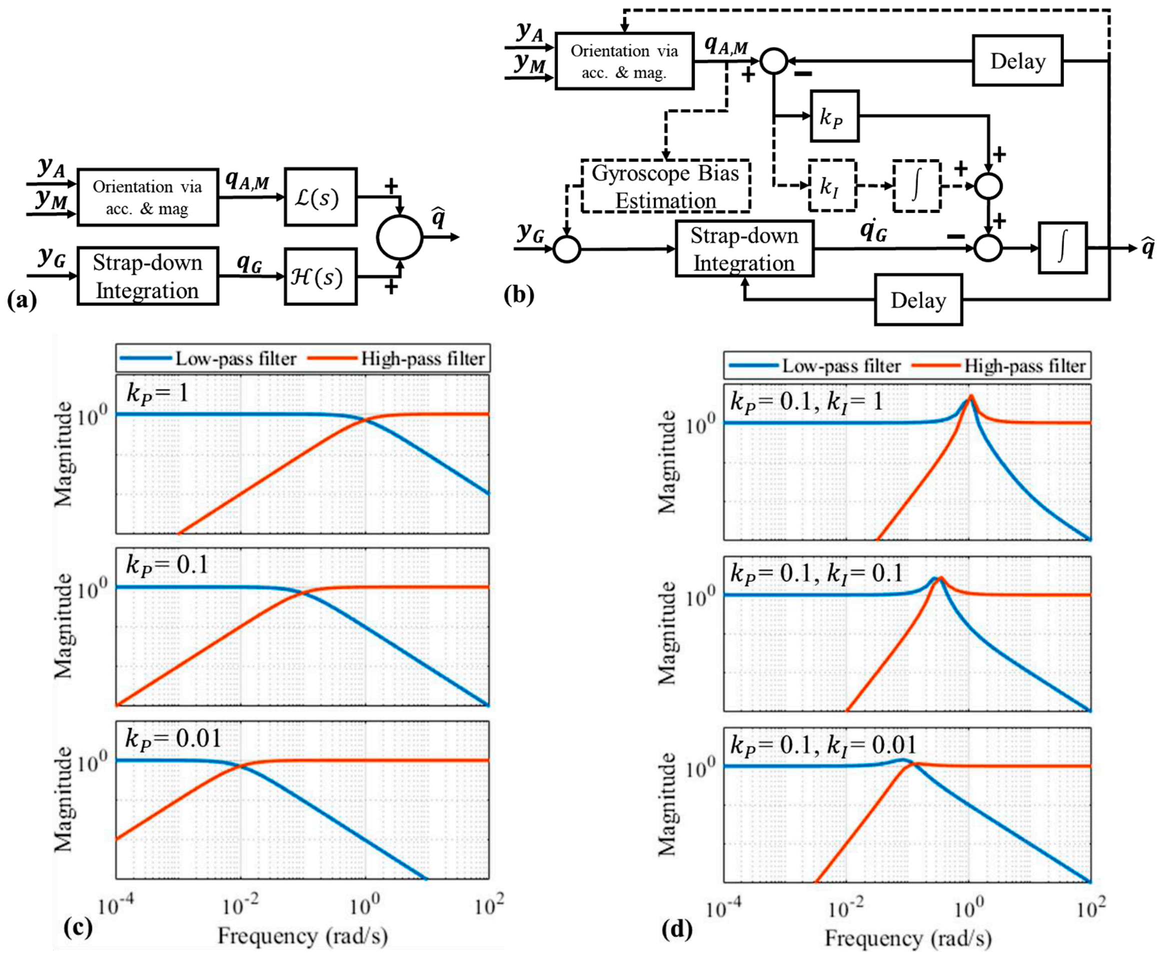


**Fig. 1.** Flowchart and frequency response of a Complimentary Filter (CF). (a) The general structure of a CF; (b) Flowchart of the CF with low-pass filter transfer function defined as $\mathcal{L}(s) = \frac{C(s)}{C(s)+s}$ where $C(s) = k_P + \frac{k_I}{s}$, and $k_P$ and $k_I$ are the proportional and integral gains, respectively; (c) Frequency response of the proportional CF, (d) Frequency response of the proportional-integral CF.

before the SDI. However, one must note that $b_G$ is a function of environmental conditions, such as ambient temperature, and extra caution must be exercised when environmental conditions change drastically during data acquisition [60].

### 2.3. Vector observation (VO) algorithms

VO algorithms, commonly used in spacecraft AHRSs, provide an estimate of the rigid body absolute orientation w.r.t. to a reference frame. To this end, two or more vectors measured in the local rigid body frame, as well as their counterpart in the desired reference frame, are required. In this setting, almost all VO algorithms are based on minimizing the cost function $\mathcal{J}(A) = \frac{1}{2}\sum_i a_i|b_i - Ar_i|^2$, known as the Wahba's problem [61], where $A$ is the DCM representing the rigid body orientation (to be estimated), $b_i$ is a unit vector measured in local rigid body frame, $r_i$ is the corresponding unit vector in the reference frame, and $a_i$ is the weight associated with each VO. Markley and Mortari [62] provided an overview of the most popular algorithms for solving the Wahba's problem and compared their accuracy and speed.

For orientation tracking with MIMUs, VOs ($b_i$) are the normalized $y_A$ and $y_M$, and their reference counterparts ($r_i$) are the gravitational acceleration, ${}^G g$, and the Earth's geomagnetic field vector, ${}^G m$, respectively, where $G$ represents the Earth's reference frame. In this setting, the TRIAD algorithm calculates the DCM $A$ using (5) [34,63],

$$w_1 = b_1/|b_1|, \; w_2 = (w_1 \times b_2)/|w_1 \times b_2|, \; w_3 = w_1 \times w_2 \tag{5a}$$

$$v_1 = r_1/|r_1|, \; v_2 = (v_1 \times r_2)/|v_1 \times r_2|, \; v_3 = v_1 \times v_2 \tag{5b}$$

$$A = w_1 v_1^T + w_2 v_2^T + w_3 v_3^T \tag{5c}$$

In TRIAD, attitude is calculated using ${}^G g$ and is immune to magnetic disturbance. In contrast to TRIAD, QUEST [64] can accommodate more than two VOs by selecting proper weights $a_i$ for sensors with different accuracies. However, in QUEST, magnetic disturbance can affect the attitude estimation as well as yaw angle.

Along with TRIAD, the Factored Quaternion Algorithm (FQA) [36] was designed to decouple $y_A$ and $y_M$ and cancel the effect of magnetic disturbance on attitude calculation. TRIAD and FQA produce similar solutions to the Wahba's problem, with the exception that the former produces a DCM and the latter produces a quaternion [36]. Other variants of VO algorithms include: Davenport $q$-method [65]; fast optimal attitude matrix [66]; singular value decomposition-based method [67]; filter QUEST [68]; recursive QUEST [69]; fast linear quaternion attitude estimator [70]; recursive linear continuous quaternion attitude estimator [71]; quaternion-based iterated least-square [72]; and algebraic quaternion algorithm [73,74]. The main advantage of the VO algorithms is that they can estimate the absolute orientation. However, as the VOs ( $y_A$ and $y_M$) could be corrupted by $\mathfrak{a}$ and $\mathfrak{b}$, these algorithms are not suitable for indoor orientation tracking during highly dynamic tasks.

### 2.4. Complementary filters

#### 2.4.1. Foundations

For an accurate estimate of orientation, the accelerometer and magnetometer should be used during static conditions (low-frequency), while the gyroscope should be used during dynamic conditions (high-frequency). To do this, the CF structure includes a low-pass filter $\mathcal{L}(s)$ to remove the high-frequency estimations obtained by the accelerometer and magnetometer and a high-pass filter $\mathcal{H}(s)$ to remove the low-frequency estimations obtained by the gyroscope, as shown in Fig. 1 (a). Commonly, the two filters' structures have been selected such that $\mathcal{L}(s) = \frac{\mathcal{C}(s)}{\mathcal{C}(s)+s}$ and $\mathcal{L}(s) + \mathcal{H}(s) = 1$, where $\mathcal{C}(s)$ is a transfer function.

The simplest choice for $\mathcal{L}(s)$ and $\mathcal{H}(s)$ is a first-order low-pass and high-pass filter, respectively, with a cut-off frequency of $k_P$. To achieve this, we can set $\mathcal{C}(s) = k_P$ in $\mathcal{L}(s)$, which results in the basic CF structure shown in Fig. 1(b) with solid lines in the time domain. Fig 1(c) shows the frequency response of the basic CF for three different values of $k_P$. The optimal value of $k_P$ depends on the dynamics of motion. That is, for relatively slow motions, a larger $k_P$ is preferred while for high dynamics, a smaller $k_P$ should be chosen [75]. As shown in Fig. 1(c), the slope of the frequency response plot of the low- and high-pass filters is not steep, and thus, the filter output contains components of both filters. To address this issue, and to achieve steeper slopes with frequency responses in Fig. 1(d), we can add an integrator with gain $k_I$ to the basic CF structure, i.e., $\mathcal{C}(s) = k_P + \frac{k_I}{s}$, as shown with the dashed line in Fig. 1(b).

#### 2.4.2. Literature survey

As the SDI was used in almost all CFs developed for MIMU orientation tracking, this section is focused on various approaches for (i) estimating the orientation via accelerometer and magnetometer and (ii) low and high-pass filters' structure. See Table 2 for a comparison of CFs in the literature. Bachmann et al. [76] used the Gauss-Newton Algorithm (GNA) to modify the SDI output based on a corrective term that minimized the error between the measured $y_A$ and $y_M$ and the projection of the ${}^{G}g$ and ${}^{G}m$ in MIMU's sensor frame, SF, as in (6),

$$q_{A,M}\left({}^{SF}_{G}\widehat{q}_k\right) = [y_A,\ y_M] - \left[{}^{SF}_{G}\widehat{q}_k^{\,*} \otimes {}^{G}g \otimes {}^{SF}_{G}\widehat{q}_k, {}^{SF}_{G}\widehat{q}_k^{\,*} \otimes {}^{G}m \otimes {}^{SF}_{G}\widehat{q}_k\right] \tag{6}$$

where ${}^{SF}_{G}\widehat{q}$ is the orientation of the MIMU sensor frame w.r.t. the Earth's reference frame, * and $\otimes$ are the quaternion conjugate and multiplication operations, respectively. Close variants of the same approach have been used in other works, including fast quaternion-based orientation optimizer [77]; Gradient Descent Algorithm (GDA)-based CF [25]; Levenberg-Marquardt algorithm-based CF [48,78,79]; GNA-based adaptive-gain CF [80]; geometrically-intuitive CF [81]; adaptive quaternion-based CF [82]; generalized linear quaternion-based CF [83]; and others [84–90].

The CF structure shown in Fig. 1(b) has been extensively revisited in the literature [26,75,91–95]. For instance, Calusdian et al. [75] used the proportional gain $k_P$ to correct the SDI output using the weighted error between the estimated orientations by CF at the previous time instant and the FQA. In CF proposed by Lai et al. [91], first, attitude was estimated using $y_A$ as in (7),

$$roll_{acc} = \tan^{-1}\left(y_{A,y} / y_{A,z}\right),\ pitch_{acc} = \tan^{-1}\left(y_{A,x} \Big/ \sqrt{{y_{A,y}}^2 + {y_{A,z}}^2}\right) \tag{7}$$

then, the proportional-integral CF in Fig. 1(b) was employed to correct the SDI output. Similarly, Liu and Zhu [111] proposed a CF based on the proportional-integral and multi-sample rotation vector concepts to eliminate the cumulative and noncommutativity errors of SDI in high dynamics.

Mahony et al. [26] formulated the CF as a deterministic observer posed on the special orthogonal group $SO(3)$. The proposed explicit CF does not require an algebraic reconstruction of the attitude, as in VO algorithms, and due to its low computational complexity, is ideal for embedded hardware platforms. Also, the explicit CF can work with only one VO ( $y_A$ or $y_M$). Similarly, Khosravian and Namvar [96] presented a nonlinear observer with asymptotic convergence based ona single VO ( $y_A$ or $y_M$). In general, a single VO can be used along with a thresholding scheme as in [88,93] (also known as vector selection [51,77]), or with fuzzy logic [97,98], to reject imperfect measurements, such as rejecting $y_A$ during high dynamic tasks or $y_M$ during magnetic disturbance.

The stability properties of the explicit CF proposed in [26] were proven when the reference vectors are (i) stationary or (ii) time-varying but the $y_G$ is bias-free. Later, Grip et al. [99] proposed an improved explicit CF for cases when the reference vectors are time-varying and $y_G$ is corrupted by bias. Also, Jensen [100] proposed a generalized version of the explicit CF by replacing the constant scalar gains by time-varying matrix gains. Because the gain tuning procedure for the explicit CF was based on trial-and-error, to provide a Kalman-like gain tuning capability for the filter, De Silva et al. [101] proposed the right-invariant formulation for the explicit CF with an intuitive gain tuning procedure based on the system's noise parameters.

Martin and Salaun [49] and Hua et al. [102] developed nonlinear observers by decoupling the yaw angle estimation from attitude estimation to minimize the effect of $\mathfrak{d}$ on attitude. Fan et al. [103] and Wu et al. [104] proposed quaternion-based two-step CFs (step 1: estimate attitude by fusing $y_G$ and $y_A$, step 2: estimate yaw using $y_M$). This allowed them to make attitude estimations immune to $\mathfrak{d}$ and enable the filter to use two separate gains to minimize the effect of $\mathfrak{a}$ and $\mathfrak{d}$ in steps 1 and 2, respectively. Valenti et al. [73] introduced a VO algorithm for solving the Wahba's problem without singularity and, accordingly, developed a quaternion-based CF with attitude estimation immune to $\mathfrak{d}$. Marantos et al. [105] developed a CF based on a new analytical solution for Wahba's problem complemented with a gyroscope propagation and an adaptive gain regulation scheme to provide smooth orientation tracking in high dynamics. Yang et al. [106] formulated a linearly discrete dynamic model to relate the attitude to $y_A$ and then developed a computationally efficient adaptive gain CF to combine the estimated attitude with SDI output.

Chang et al. [107] first developed a smooth sliding-mode observerfor attitude estimation using $y_A$, and then improved the observer estimations byincluding measurement noise and biases [108]. El Hadri and Benallegue [109] proposed a nonlinear sliding-mode CF to achieve robust orientation tracking and $b_G$ estimation under parametric uncertainties and modelling errors. Vasconcelos et al. [110] introduced a CF using Euler angle parametrization (stable for non-singular configurations) and $b_G$ compensation and tuned the filter gains in the frequency domain to account for unmodeled disturbances found in the experimental setup. By estimating a virtual angular velocity for the rigid body using $y_A$ and $y_M$, Tayebi et al. [111] developed a quaternion-based CF to track the orientation as well as an asymptotic estimate of $b_G$. Sheng and Zhang [112] proposed the application of a neural network-based proportional-integral-derivative controller for calculation of $b_G$ based on the error between estimated orientation by SDI and a VO algorithm. In the nonlinear CF introduced by Wu et al. [113], the error between $y_A$ and the projection of ${}^{G}g$ in MIMU sensor frame was used to estimate the $b_G$ and correct the angular velocity before SDI. However, this method does not provide an estimate of $b_G$ when the MIMU is motionless or $y_A$ is parallel to ${}^{G}g$.

#### 2.4.3. Modified complementary filters

Because the performance of a CF highly depends on its gains, Alves Neto et al. [114] proposed a CF using Euler angle parametrization and adaptive gains with values proportional to exp(-$|{}^{G}g$- $||y_A|||$). Kottath et al. [115] presented the application of an ensemble of linear CFs with different gains to minimize the effect of gain value on the estimated orientation. In the proposed ensemble, the weighting factor associated with each CF was adaptively calculated based on the difference between

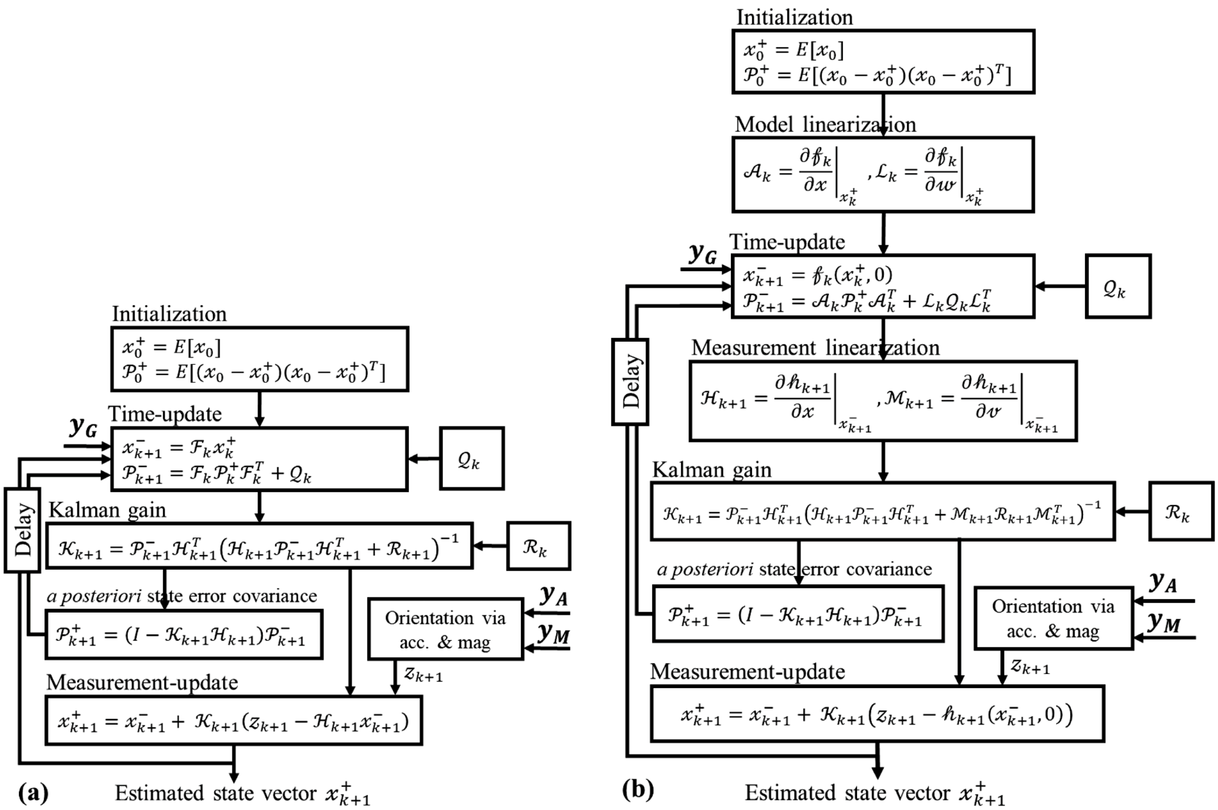


**Fig. 2.** Flowchart of a general (a) Linear Kalman Filter and (b) Extended Kalman Filter. $\mathfrak{x}$ is the state vector, $\mathfrak{z}$ is the measurement vector. $\mathcal{P}$ is the state error covariance matrix. $\mathcal{F}$ and $\mathfrak{f}(\cdot)$ are the state transition matrix and equation, respectively. $\mathcal{H}$ and $\mathfrak{h}(\cdot)$ are the measurement prediction matrix and equation, respectively. $\mathcal{Q}$ and $\mathcal{R}$ are the system and measurement model covariance matrices, respectively. $\mathcal{K}$ is the Kalman gain.

the CF's and the ensemble's estimates. To adaptively compute the CF gains based on the error between the orientation obtained from $y_A$ and $y_M$ and CF output, Poddar and Narkhede [116] developed a non-linear CF aided with a Particle Swarm Optimization (PSO) gain tuning scheme. It should be noted that the application of an adaptive gain tuning scheme or thresholding method for rejecting $\mathfrak{a}$ and $\mathfrak{d}$ cannot guarantee an accurate and robust estimation. For example, if gain tuning is used for an extended period of time to cancel the estimation errors from $y_A$ during high dynamics, drift in attitude estimations will eventually occur because of $b_G$.

### 2.5. Kalman filters

#### 2.5.1. Foundations

Suppose that we describe the orientation tracking problem using linear or nonlinear discrete-time systems in (8a) and (8b), respectively,

$$\mathfrak{x}_{k+1} = \mathcal{F}_k \mathfrak{x}_k + \mathcal{B}_k \mathfrak{u}_k + \mathfrak{w}_k$$

$$\mathfrak{z}_{k+1} = \mathcal{H}_{k+1} \mathfrak{x}_{k+1} + \mathfrak{v}_{k+1} \tag{8a}$$

$$\mathfrak{x}_{k+1} = \mathfrak{f}_k(\mathfrak{x}_k, \mathfrak{u}_k, \mathfrak{w}_k)$$

$$\mathfrak{z}_{k+1} = \mathfrak{h}_{k+1}(\mathfrak{x}_{k+1}, \mathfrak{v}_{k+1}) \tag{8b}$$

where $\mathfrak{x}$, $\mathfrak{u}$, and $\mathfrak{z}$ are states of the system (commonly the MIMU orientation), input to the system (commonly $y_G$), and sensor measurements (commonly $y_A$ and $y_M$), respectively; $\mathfrak{w}$ and $\mathfrak{v}$ are white Gaussian noise processes associated with system and measurement models with covariances $\mathcal{Q}$ and $\mathcal{R}$, respectively; $\mathcal{F}$ and $\mathfrak{f}(\cdot)$ are the state transition matrix and equation, respectively (also known as state propagation); and $\mathcal{H}$ and $\mathfrak{h}(\cdot)$ are the measurement prediction matrix and equation, respectively. Now, suppose that we show the estimation error, i.e., the error between the true state and the estimated state, of the linear system in (8a) by $\tilde{\mathfrak{x}}$ and our aim is to find the estimator that minimizes the weighted 2-norm of the expected value of $\tilde{\mathfrak{x}}$, i.e., $\min E[\tilde{\mathfrak{x}}^T \mathcal{T} \tilde{\mathfrak{x}}]$, where $\mathcal{T}$ is a positive definite weighting matrix. Then:

- If $\mathfrak{w}_k$ and $\mathfrak{v}_k$ are uncorrelated zero-mean white Gaussian processes, KF is the solution.
- If $\mathfrak{w}_k$ and $\mathfrak{v}_k$ are uncorrelated zero-mean white processes, KF is the best linear solution.
- For other cases, such as correlated/coloured noise or nonlinear system in (8b), the KF can be modified to answer the above problem [117].

In other words, the aim of using a KF is to estimate the state vector, $\mathfrak{x}$, based on our knowledge of the system model and the availability of the noisy input, $\mathfrak{u}$, and measurements, $\mathfrak{z}$. To this end, we can use LKF and EKF, as shown in Fig. 2(a) and (b), to estimate the orientation using the linear and nonlinear systems in (8a) and (8b), respectively [117].

For orientation tracking applications, the rigid body orientation is commonly considered to be the state vector. Also, (i) the SDI is used to model the time-update equation, i.e., $\mathcal{F}$ or $\mathfrak{f}(\cdot)$; and (ii) the difference between the measured and estimated acceleration and geomagnetic field is used to model the measurement-update equation, i.e., $\mathcal{H}$ or $\mathfrak{h}(\cdot)$. More complex KFs have been introduced by including $\mathfrak{a}$, $b_G$, and/or $\mathfrak{d}$ in the state vector (see Table 3 for a comparison of various KFs introduced in the literature).

#### 2.5.2. Linear Kalman filters (LKF)

Barshan and Durrant-Whyte [118] used $y_G$ to build an LKF for estimating the yaw angle of a planar mobile robot. By inspection, they found an exponential model for $b_G$ during the warm-up period and showed that the inclusion of this model reduced the estimation error by a factor of 5.

Qi and Moore [8] proposed an LKF for GPS/MIMU data fusion, where the GPS readouts were taken as the LKF measurements, and MIMU readouts were taken as the additional information required for state propagation. Yun et al. [119] and Yean et al. [120] introduced LKFs where SDI was used to build the time-update equation and the error between $y_A / y_M$ and the projection of ${}^G g / {}^G m$ in MIMU sensor frame, as in (6), along with GNA and GDA were used to construct the measurement-update equation. Whole and Gebhard [121] extended this approach by switching between calculating the gradient of $y_A$ and $y_M$ under homogenous magnetic condition to calculating the gradient of $y_A$ only under magnetic disturbance.

Lee and Park [122] used the optimal two-observation quaternion estimation method proposed in [123] along with a vector selection technique to estimate the orientation from $y_A$ and $y_M$ under quasi-static motions in magnetically homogeneous conditions and correct the predicted orientation by SDI in an LKF structure. Seo et al. [124] proposed the application of the FQA to calculate the orientation using $y_A$ and $y_M$ and correct the SDI output in a standard LKF. They also suggested a correction scheme using quaternion linear interpolation to combine the LKF and FQA outputs during static conditions which would eliminate the effect of $b_G$. Similarly, Valenti et al. [74], Guo et al. [125], Feng et al. [40], and Wu et al. [71] developed new algebraic quaternion estimators using $y_A$ and $y_M$ to formulate the measurement-update equation of a standard LKF. Some of these algebraic quaternion estimators made the attitude estimation immune to magnetic disturbance while providing higher computational efficiency compared to FQA.

Kim and Golnaraghi [126] proposed a magnetometer-free LKF in which the angular velocity used in SDI and its bias were modelled as first-order Markov processes and included in the state vector. Also, the measurement-update equation was constructed using the error between (i) $y_G$ and the estimated angular velocity, $\hat{\omega}$, plus bias and (ii) $y_A$ and the projection of ${}^G g$ in MIMU sensor frame. Also, Ligorio and Sabatini [127] developed a magnetometer-free LKF to estimate the attitude from the estimated gravitational acceleration, ${}^G\hat{g}$. However, these magnetometer-free LKFs limit the tracking to attitude only. Thus, other works [128–130] proposed two separate LKFs, or dual filtering,for estimating gravitational acceleration and geomagnetic field, to compute the 3D orientation while eliminating the errors in yaw estimation from those of attitude estimation. For instance, Zhu and Zhou [28] and Zhu et al. [131] used an LKF to estimate the gravitational acceleration, ${}^G\hat{g}$, and geomagnetic filed, ${}^G\hat{m}$, by propagating the state vector using $y_G$ in time-update step and then comparing the state vector with $y_A$ and $y_M$ during measurement-update. Batista et al. [132,133] extended the previous LKF structure by including $b_G$ in the state vector and correcting the $y_G$ accordingly during the time-update step.

Jurman et al. [134] constructed an adaptive LKF with Euler angles in its state vector. In this LKF, the state vector was propagated in time using SDI and the Euler angles calculated from $y_A$ (using (7) for attitude) and $y_M$ (using $\tan^{-1}(y_{M,y}/y_{M,x})$ for yaw) were used as the measurements. Sun et al. [135] included $\mathfrak{a}$ with a first-order Markov process model in the state vector of their proposed LKF and used the modified acceleration (${}^G g$ ++ estimated $\mathfrak{a}$) in (6) to build the measurement-update equation. In another approach, instead of an explicit modeling of $\mathfrak{a}$, Makni et al. [136,137] proposed an adaptive LKF where the part of $\mathcal{R}$ associated with the accelerometer was estimated adaptively in real-time based on the LKFs accelerometer residual. Also, the proposed LKF was structured with energy consumption considerations in mind such that the gyroscope was turned-off and re-activated alternately while the $\mathcal{Q}$ was adaptively tuned to compensate for the errors. Also, Rehbinder and Hu [138] proposed an SFA by switching between two LKFs similar to the high gain observer previously proposed by the same authors in [139], i.e., one for tracking under low accelerations and one for high accelerations.

*2.5.3. Extended Kalman filters (EKF)*

Lefferts et al. [140] investigated the effect of constructing an EKF with different variations of quaternions as the state vector and concluded that including all elements of the quaternions and $b_G$ could lead to singularity in calculating $\mathcal{Q}$. Koifman and Merhav [141] proposed the application of an EKF for real-time attitude estimation using $y_G$ and $y_M$, investigated the effect of piecewise constant modelling of $b_G$ on estimation error, and then devised a method for updating the corresponding elements of the covariance matrix when required. Vaganay and Aldon [142] proposed an EKF in which the state vector included roll and pitch angles as well as their drift rates, while the SDI was performed out of EKF and as a part of the measurement-update.

Marins et al. [143] and Yun and Bachmann [29,144] investigated two approaches for EKF design using different measurement vectors: (i) using MIMU readouts as the measurement; and (ii) using the orientation (in quaternion) obtained by applying GNA or QUEST to $y_A$ and $y_M$. They showed that in the former, the measurement-update equations were highly nonlinear functions of the state vector while in the latter, linear equations could be used to relate measurements to the state vector, which made the EKF suitable for real-time applications due to lower computational complexity. Also, Mazza et al. [145] introduced a similar magnetometer-free EKF but included $b_G$ in the state vector. Sabatini [51] and Zhang et al. [146] included the accelerometer and magnetometer bias terms in the state vector of their proposed EKF and used their estimated values to correct the projection of ${}^G g$ and ${}^G m$ in MIMU sensor frame during calculation of the predicted measurements.

Also, Sabatini [147] developed a similar EKF by substituting the bias terms in the previous EKF by $b_G$ and $\mathfrak{d}$. Later, Sabatini [148] extended this work by introducing a variable-state-dimension EKF. This EKF switched between an EKF where a first-order Markov process was used to model $\mathfrak{d}$ and a higher-order EKF where a second-order Markov process modelled the time-rate of change of the magnetic field. This approach could make the propagation of state vector and calculation of the predicted measurements more realistic, particularly for long-duration tracking under magnetic disturbances. Following the same concept, Xu et al. [149] used a decision tree-based switching technique to develop an EKF capable of changing its measurement model between three modes (high $y_G$, high$y_A$, moderate $y_A$) to achieve robust tracking performance under different conditions.

*2.5.4. Complementary Kalman filters (CKF)*

While it is common to use the KF structure to estimate the primary states directly, some works proposed CKF structure, also known as the error-state KF [150,151], to estimate the errors in the primary states [6, 152]. By defining the state vector as an error process, the *a priori* estimate of the state vector is always zero, and thus, the state transition, $\mathcal{F}$ or $\mathfrak{f}(\cdot)$, is zero, which simplifies the standard KF formulation. For instance, Foxlin [153], Setoodeh et al. [154], and Gebre-egziabher et al. [155] proposed CKFs by estimating the errors in gyroscope bias and Euler angles to correct $y_G$ and the SDI output before and after the SDI, respectively. Gebre-egziabher et al. [155] also used the quaternion errors to develop a similar CKF and showed that the quaternion parametrization has advantages such as more efficient gain tuning process and computations as compared to Euler angle parametrization. To achieve more robust estimates for indoor orientation tracking, Zhang and Reindl [156] added a magnetic disturbance rejection step to the CKF by Foxlin [153].

Roumeliotis et al. [150] introduced a smoothing filter, comprised of two CKFs, where the first CKF propagated the attitude estimate forward and then updated it via the absolute orientation obtained from the accelerometer and sun sensor, while the second CKF propagated the most recent estimate back in time to lower the uncertainty of the estimation. To estimate the errors in the attitude of a mobile robot moving on uneven terrains using $y_A$ and the SDI, Fuke and Krotkov [157] proposed the application of a CKF. Luinge and Veltink [54] developed an

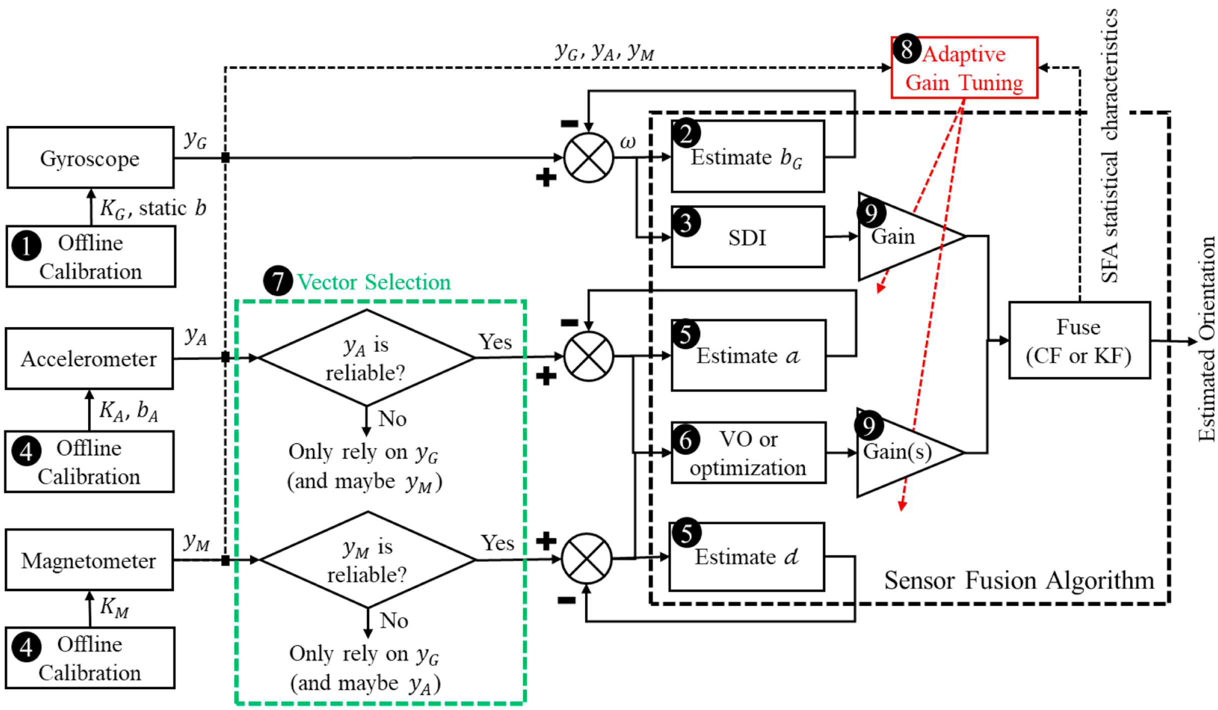


**Fig. 3.** Flowchart of a general sensor fusion algorithm (SFA) containing offline calibration of sensors, vector selection for imperfect measurement rejection, and adaptive gain tuning.

accelerometer-based CKF to estimate the error in gravitational acceleration and accelerometer offset by deriving the relationship between $y_A$ and the state vector as well as calculating the angular velocity based on the direction of the $y_A$ at each two successive time instants. Luinge and Veltink [59] also used both accelerometer and gyroscope to estimate the orientation error and gyroscope bias using the CKF structure. Later, the magnetometer was included in the CKF to prevent drift in the yaw angle, even under magnetic disturbances [52].

Hall et al. [158] proposed a CKF where $y_G$ was used to propagate the error in orientation while $y_A$ and GPS were used to perform the measurement-update. However, as the accelerometer and GPS had different sampling rates and reference frames, the proposed CKF took advantage of the incremental update concept [159], where the measurement-update could be performed independently for each sensor. Kang et al. [160] developed a CKF to fuse a gyroscope and a vision system where a fading factor, tuned using fuzzy logic, has been applied to the Kalman gain, $\mathcal{K}$, to tune the tracking performance of the filter in response to the quality of the vision system data. Kannan [161] proposed a linear CKF where the compensation of the drift in the estimated orientation was performed via the time-update equation (using the orientation obtained by TRAID from $y_A$ and $y_G$) instead of the measurement-update equation. This approach resulted in a substantial improvement of the response and settling times of the proposed CKF.

### 2.5.5. Modified Kalman filters

Ren and Kazanzides [162,163] proposed a two-layer filtering scheme such that two LKFs in the first layer were designed to estimate ${}^G\hat{g}$ and ${}^G\hat{m}$ from $y_A$ and $y_M$, respectively, and an EKF in the second layer was used to correct the predicted orientation by SDI using the orientation calculated by VOs from the first layer. Music et al. [164] introduced a two-layer filter where in the first layer, a standard EKF estimated orientation using SDI and direct Euler angle calculation from $y_A$ and $y_M$, while the estimated orientation in the second layer (calculated using a Particle Filter) was used to present extra information to EKF and improve the overall performance. Sabatelli et al. [165] developed a two-layer filter where the first and second layers used $y_A$ and $y_M$, respectively, to correct the propagated orientation by the SDI. Also, Dang and Nguyen [166] proposed a two-layer filter where in the first layer, an EKF estimated the third column of DCM (associated with attitude) and $\mathfrak{a}$ while in the second layer, an EKF with similar structure estimated the first column of DCM (associated with yaw angle) and $\mathfrak{d}$. Such structures have the benefit of eliminating the effect of magnetic disturbance from the attitude estimations.

### 2.5.6. Adaptive gain tuning of Kalman filters

KF performance highly relies on an accurate definition of the system and measurement models, as well as noise covariance matrices (commonly, $\mathcal{Q}$ and $\mathcal{R}$ are defined before the estimation starts and remain fixed during the tracking process). However, in reality, $\mathcal{Q}$ and $\mathcal{R}$ could change over time due to the time-varying nature of the errors, such as orientation tracking during slow (quasi-static) and fast motions. Therefore, adaptive KFs have been proposed to respond to the changes in the nature of the error by tuning $\mathcal{Q}$ and $\mathcal{R}$ in real-time [167].

For example, in the covariance scaling technique, $\mathcal{Q}$ or $\mathcal{R}$ are scaled by the factor $\mathcal{S}_k > 1$ to put more weight on the *a priori* state vector $\mathfrak{x}^-$, or measurements, respectively [168]. $\mathcal{S}_k$ can be tuned using the magnitude of $y_A$, $y_G$, and/or $y_M$ at some predefined levels [51,145], or the magnitude of the predicted residuals [168]. For example, Suh [55] and Suh et al. [169] customized the application of the covariance scaling technique for a CKF and EKF, respectively, such that instead of applying a small $\mathcal{S}_k$ to all elements of $\mathcal{Q}$ or $\mathcal{R}$ to guard against $\mathfrak{a}$ (and rely more on $y_G$), first, the direction of the $\mathfrak{a}$ was estimated, and small weights were supplied only for the affected axes. Sun et al. [170] included an adaptive scheme in their standard CKF to weight $\mathcal{R}$ based on the error between magnitude and direction of $y_A$ ($y_M$) with its reference value recorded during static (magnetically undisturbed) condition. Later, this method was extended by Johnson and Sathyan [171] to include $b_G$ estimation. Tong et al. [172] proposed the application of a hidden Markov Model recognizer to identify the measurement disturbances and adjust $\mathcal{R}$ of their proposed CKF adaptively. Also, Jamil et al. [173] used an Artificial Neural Network to eliminate the errors in $y_A$ and $y_G$ by adjusting $\mathcal{R}$.

In the innovation-based adaptive estimation technique, the innovation sequence, that is, the difference between the real measurement and its predicted value by the KF, is used in an algorithm known as the covariance matching to tune the value of $\mathcal{Q}$, $\mathcal{R}$, or $\mathcal{K}$ such that the actual value of the innovation sequence covariance matrix matches its theoretical value [174,175]. Finally, in the multiple-model adaptive estimation technique, a bank of KFs (each using a different $\mathcal{Q}$ or $\mathcal{R}$) runs in parallel to calculate the *a posteriori*state estimate $\mathfrak{x}^+$ based on the weighted combination of the predicted state by each KF (KF weights could be obtained based on the probability density function of the innovation sequence covariance matrix) [176].

## 3. Discussion

Over the past forty years, researchers have developed various SFAs for orientation tracking with MIMUs. KFs and CFs were used to compensate for the limitations associated with the SDI or VO algorithms. In both KF and CF approaches, the SDI of $y_G$ was used to propagate the orientation in time, and then, the propagated orientation was corrected with the orientation estimated by a VO algorithm or a corrective term obtained by an optimization rule such as GDA. However, technical differences were observed amongst these SFAs, even amongst those in the same family. Therefore, we conducted a survey study to (i) review and categorize publications in this field to help researchers acquire an inclusive understanding of the technical developments; (ii) aggregate the lessons learned from the previous works to help researchers developing novel SFAs; and (iii) summarize the main challenges that are needed to be addressed in future. The first task was done in Section 2 of the current survey, while the second and third tasks were addressed in Sections 3.1 and 3.2, respectively.

### 3.1. Lessons learned

Numerous works proved the efficiency of SFAs in compensating the limitations associated with the SDI or VO algorithms for orientation tracking with MIMUs. In this section, we listed the lessons learned during the literature survey. The general flowchart of an SFA in Fig. 3 includes features that could improve the accuracy and robustness of the orientation estimation.

#### 3.1.1. Gyroscope and strap-down integration (SDI)

SDI of $y_G$ is the core of almost all CFs and KFs. Therefore, the accuracy of the propagated orientation in time via SDI is vital to the accuracy and robustness of any SFA, especially when aiding sensors' recordings, i.e., $y_A$ and $y_M$, are not reliable, such as tracking under high dynamics or magnetically disturbed environments. To improve the accuracy of SDI, the followings must be considered.

(i) Use a gyroscope with low bias.
(ii) Correct the gyroscope's static bias and scale factor (block 1 in Fig. 3). For the static bias, before any data acquisition, the MIMU must be turned on and put at rest for a while (commonly specified by the manufacturer, and if not, at least 20 minutes according to [42]). This will ensure that the gyroscope has reached ambient temperature, and the estimated static bias will not change significantly due to temperature change. Then, $y_G$ must be measured when the MIMU is at rest to obtain an estimate of the static bias. Finally, the estimated static bias must be removed from $y_G$ recorded during data acquisition.
(iii) Use stochastic models [52,147] or heuristics [41] to estimate the time-varying $b_G$ in real-time (block 2 in Fig. 3). A first-order Markov process, as in (1b), can be used for this purpose. According to the principle of pseudo-noise injection, estimating $b_G$ can improve the accuracy and robustness of the orientation tracking, even for short trials where $b_G$ does not have time to change drastically [127].
(iv) Use an accurate estimation of $\exp(\cdot)$ for the SDI in (4a) (block 3 in Fig. 3). For example, using a first-order Taylor series showed inaccurate results under low sampling frequencies [57].

#### 3.1.2. Accelerometer and magnetometer

During long-duration trials, the use of accelerometer and magnetometer are crucial to an SFA, as they can correct the cumulative error of the SDI. Thus, consider the following for these aiding sensors.

(i) Evaluate the calibration of these sensors (blocks 4 in Fig. 3). Various procedures have been introduced in the literature to verify and possibly re-calibrate accelerometers [27,53,177] and magnetometers [178]. These procedures use *ad hoc* tests to estimate the scale factors $K_A$ and $K_M$ (in (2a) and (3a)), as well as the bias terms of these sensors, which can be later used to correct $y_A$ and $y_M$.
(ii) Use online stochastic models, e.g., first-order Markov processes as in (2b) and (3b), to estimate $\mathfrak{a}$ and $\mathfrak{d}$, respectively, and correct $y_A$ and $y_M$ (blocks 5 in Fig. 3). This correction is effective for motions with high dynamics or in magnetically disturbed environments [51,52,127].

#### 3.1.3. Dealing with magnetic disturbance

Magnetic disturbance can significantly affect the yaw angle estimation, which in turn may affect the attitude estimation. Thus, consider the following when formulating an SFA.

(i) Decouple the attitude estimation from $y_M$ or yaw angle (block 6 in Fig. 3). For example, use TRIAD, instead of QUEST, as the VO algorithm in CF or KF, or use two-layer filters as in [79,104,130,179,180].
(ii) Use vector selection to detect and reject imperfect measurements (block 7 in Fig. 3). When the geomagnetic field is disturbed, the field strength and dip angle change significantly. Therefore, magnetic disturbance can be identified by applying thresholds to the field strength and/or dip angle. In such cases, the propagated orientation by SDI can be declared as the estimated orientation without any correction, see [38] for more details. A similar approach can be applied to $y_A$ to reduce the effect of non-gravitational acceleration.

#### 3.1.4. Adaptive gain tuning

Gain tuning plays a significant role in the performance of any SFA; if gains are selected improperly, the SFA could even diverge. Therefore, consider the following regarding SFA gains.

(i) Use an online gain turning strategy to adaptively put more weight on the most reliable source of information (block 8 in Fig. 3). For instance, to reduce the effect of correction via the magnetometer and rely more on the gyroscope, when the magnetic disturbance is detected using a vector selection, the CF gain or KF measurement covariance matrix should be adjusted accordingly.
(ii) Decouple the gains associated with gyroscope, accelerometer, and magnetometer (blocks 9 in Fig. 3). Generally, developing a KF with a different gain for each sensor is easy. However, in most well-recognized CFs, such as [25,26], the same gain is used to weight accelerometer and magnetometer. In such cases, both sensors will be declared reliable or unreliable at the same time, while one can be more reliable than the other one.
(iii) Select the filter gains rigorously. Although filter gains found by trial-and-error might result in acceptable estimations under certain working conditions, the filter performance will not be guaranteed for other situations. Therefore, filter gains must be evaluated under various motion patterns, intensities, and durations.

**Table 2**
Review of the state-of-the-art sensor fusion algorithms with a Complimentary Filter (CF) structure, including linear CF (LCK) and nonlinear CF (NCF). Abbreviations used in the table are described in the table footnotes.

| Study | Year | Application | Method | Parametrization | $b_G$, $\mathfrak{a}$, $\mathfrak{d}$ compensation | Notes (gain tuning or thresholding, etc.) |
|---|---|---|---|---|---|---|
| [76] | 1999 | HMT | GNA+CF | Q | - | - |
| [193] | 2003 | STC | NCF | Q | $b_G$ | - |
| [184] | 2006 | AVTC | NCF | DCM | $b_G$ | - |
| [111] | 2007 | - | NCF | Q | $b_G$ | - |
| [26] | 2008 | RATC | NCF | DCM | $b_G$ | - |
| [94] | 2008 | AVTC | NCF | Q | $b_G$ | - |
| [114] | 2009 | MRTC | LCK | EA | - | $k_p \propto \exp(-\lvert{}^G g - \lVert y_A \rVert\rvert)$ |
| [109] | 2009 | - | Sliding mode observer | EA | $b_G$ | - |
| [77] | 2009 | HMT | GNA+CF | Q | - | $\mathfrak{a}$ & $\mathfrak{d}$ rejection with thresholding |
| [87] | 2009 | - | Azimuth-level detector CF | Q & DCM | - | - |
| [49] | 2010 | AVTC | NCF | Q | $b_G$ | - |
| [91] | 2010 | - | NCF | EA | - | - |
| [25] | 2011 | HMT | GDA+CF | Q | - | - |
| [75] | 2011 | - | FQA+CF | Q | - | - |
| [78] | 2011 | Bio-logging | LMA+CF | Q | - | - |
| [110] | 2011 | SVTC | LCK | EA | - | - |
| [100] | 2011 | - | NCF | DCM | $b_G$ | Time-varying gains |
| [92] | 2011 | MRTC | NCF | EA | $b_G$ | - |
| [93] | 2011 | SVTC | NCF | EA | $b_G$ | CF gain $\propto \lvert{}^G g - \lVert y_A \rVert\rvert$ |
| [96] | 2012 | STC | NCF | DCM | - | - |
| [99] | 2012 | AVTC | NCF | DCM | $b_G$ &$b_A$ | - |
| [194] | 2012 | - | LCK | DCM | - | Using inverse sensor models to widen the frequency range |
| [195] | 2012 | - | TRIAD+LCK | DCM | $b_G$ | - |
| [196] | 2012 | HMT | GDA+CF | Q | $b_G$ | - |
| [197] | 2012 | HMT | LCK | DCM | - | CF gain ∝ duration of the experiment |
| [198] | 2012 | MRTC | NCF | Q | - | - |
| [97] | 2015 | - | TRIAD+NCK | DCM | - | Adaptive gain tuning using fuzzy logic |
| [80] | 2013 | HMT | GDA+CF | Q | $b_G$ | $\mathfrak{a}$ & $\mathfrak{d}$ rejection with thresholding |
| [79] | 2014 | HMT | Two-layer LMA+CF | Q | - | - |
| [41] | 2011 | HMT | GDA+CF | Q | $b_G$ | - |
| [199] | 2014 | AVTC | PI controller+CF | EA | - | - |
| [102] | 2014 | AVTC | NCF | DCM | $b_G$ | - |
| [98] | 2014 | HMT | LCK | EA | - | Adaptive gain tuning using fuzzy logic |
| [200] | 2014 | HMT | LCK | DCM | $b_G$ | - |
| [89] | 2015 | Bicycle crank angle tracking | NCF + vertical acceleration update | Q | - | - |
| [112] | 2015 | AVTC | LCK | DCM | $b_G$ estimation by neural network PID controller | - |
| [107] | 2015 | AVTC | Smooth 2nd order sliding mode observer | EA | - | - |
| [88] | 2015 | HMT | GDA+CF | Q | - | $\mathfrak{d}$ rejection with thresholding |
| [73] | 2015 | AVTC | AQA+CF | Q | - | $\mathfrak{a}$ rejection using LERP or SLERP + adaptive gain tuning |
| [201] | 2015 | AVTC | NCF | DCM | - | - |
| [81] | 2016 | HMT with smartphone | Geometrically-intuitive CF | Q | - | - |
| [104] | 2016 | - | Two-layer LCK | Q | - | $\mathfrak{d}$ rejection with thresholding |
| [105] | 2016 | AVTC | Nonlinear SVD+CF | DCM | - | - |
| [113] | 2016 | RATC | NCF | DCM | $b_G$ | - |
| [82] | 2017 | - | GDA+CF | Q | - | $\mathfrak{d}$ rejection with thresholding |
| [115] | 2017 | AVTC | LCK | EA | $b_G$ | Combining output of multiple fixed-gain CFs with MMAE |
| [116] | 2017 | AVTC | NCF | EA | - | Adaptive gain turning via PSO |
| [84] | 2018 | - | GDA+CF | Q | - | $\mathfrak{d}$ rejection with thresholding |
| [103] | 2018 | HMT | LCK | Q | - | $\mathfrak{a}$ & $\mathfrak{d}$ rejection with finite state machine |
| [85] | 2018 | RATC | FQA+CF | Q | - | Adaptive gain turning via GDA |
| [108] | 2018 | AVTC | Smooth 2nd order sliding mode observer | EA | $b_G$ | - |
| [101] | 2018 | AVTC | Right invariant NCF | Q & DCM | $b_G$ | CF gain ∝ system noise parameters |
| [106] | 2018 | AVTC | LCK | Q | - | CF gain ∝ $\lVert y_G \rVert$ |
| [202] | 2018 | - | MSRVA+CF | Q | $b_G$ | - |
| [86] | 2018 | - | GDA+CF | Q | - | - |
| [83] | 2019 | AVTC | GDA+CF | Q | - | $\mathfrak{a}$ & $\mathfrak{d}$ rejection with thresholding |
| [90] | 2019 | - | GDA+CF | DCM | $b_G$ | - |

(*continued on next page*)

**Table 2** (*continued*)

| Study | Year | Application | Method | Parametrization | $b_G$, 𝔞, 𝔡 compensation | Notes (gain tuning or thresholding, etc.) |
|---|---|---|---|---|---|---|
| [203] | 2019 | Robot teleoperation | GDA+CF | Q | $b_G$ | - |
| [95] | 2019 | AVTC | NCF | EA | $b_G$ | Identified reliable $y_G$ based on interquartile range of $y_G$ previous samples |
| [204] | 2020 | HMT | GDA+CF | Q | - | 𝔡 rejection |
| [205] | 2020 | HMT | GDA+CF | Q | - | $y_G$ rejection during "no motion" state |
| [206] | 2020 | HMT | Two-layer LCK | Q | - | - |
| [207] | 2020 | - | LCF | Q | - | - |
| [208] | 2020 | AVTC | NCF | Q | - | 𝔞 compensation by thresholding |
| [209] | 2020 | HMT | Extended CF | Q | $b_G$ | 𝔡 rejection with thresholding |

**- Application:** STC: Spacecraft (satellite) tracking/control; HMT: Human motion tracking; MRTC: Mobile robot tracking/control; RATC: Robotic arm tracking/control; AVTC: Aerial vehicle tracking/control; SVTC: Surface vehicle tracking/control.
**- Method:** GNA: Gauss-Newton algorithm; GDA: Gradient descent algorithm; LMA: Levenberg-Marquardt algorithm; FQA: Factored quaternion algorithm; AQA: algebraic quaternion algorithm; LERP: Linear intERPolation; SLERP: Spherical Linear intERPolation; SVD: Singular value decomposition; PSO: Particle Swarm Optimization; MSRVA: Multi-sample rotation vector algorithm; MMAE: Multiple-model adaptive estimation.
**- Parametrization:** Q: Quaternion parametrization of orientation; EA: Euler angle parametrization of orientation; DCM: Direction cosine matrix parametrization of orientation.
**- Compensation:** $b_G$: Gyroscope bias; $b_A$: Accelerometer bias; 𝔞: external non-gravitational acceleration; 𝔡: magnetic disturbance.

#### 3.1.5. Beyond EKF

Violation of the assumptions that were used to formulate a filter can degrade its performance. Thus, consider the following two extensions for KFs.

(i) When execution time is not a consideration, use unscented KF instead of EKF. As EKF uses linearization to propagate the mean and covariance of the state vector, its performance can deteriorate for highly nonlinear systems.
(ii) Use robust filtering techniques when adaptive gain tuning is not possible. For example, the -$H_\infty$ filter formulates an estimation strategy that bounds the worst-case estimation error by adaptively weighting the state error covariance matrix [117]. Also, the -$H_\infty$ filter assumes that the process and measurement noises are energy bounded signals, and drops the Gaussian distribution assumption for noises in formulating the standard KF.

### 3.2. Future research challenges

Various VO/CF/KF formulations with major or minor differences have been developed for orientation tracking with MIMUs. Thus, one could argue that technical contribution to this field is not the primary research challenge at the moment. Instead, we suggest that test platforms [181] and benchmarking studies are required to identify the most effective SFAs, as well as techniques that could improve the accuracy and robustness of SFAs. The reason is that each publication assessed the performance of its proposed SFA using limited test scenarios in terms of motion duration, pattern, and intensity. Also, other contributing factors, such as the manufacturing quality of the MIMU or optimal SFA gains, were not considered in assessments. As a result, contradictory results on the performance of SFAs have been reported in various studies.

Therefore, developing benchmarks where SFAs can be assessed against each other under similar testing conditions remains the main challenge in the field of orientation tracking with MIMUs. Such a benchmark must have the following features.

(i) Various test scenarios are recorded. Short- and long-duration trials are required to evaluate the effect of $b_G$. Static, medium and high dynamic (with static periods in the middle) trials are required to evaluate convergence and tracking ability of the SFAs. Extreme testing scenarios, such as MIMU impact, are required to reveal the robustness of an SFA.
(ii) The true orientation is recorded synchronously with MIMUs using a reference system such as the camera motion-capture system. This information is not only useful for performance assessment but also for tuning the SFA's gain(s).
(iii) Data of multiple MIMUs, preferably with different manufacturing qualities, are recorded. Such trials can demonstrate the effectiveness of the SFA correction strategy using the aiding sensors, specifically for long-duration trials where SDI faces a significant drift.

Using a benchmark with these features, optimal gains for each SFA and MIMU should be obtained using a portion of the data and by comparing the estimated and reference orientations. The rest of the data can be used for validation.

Finding the most effective techniques for improving the performance of the existing SFAs is the second research challenge. Using a benchmark, the following should be evaluated.

(i) Various adaptive gain tuning strategies must be assessed. While some strategies, such as the covariance scaling technique, can only be applied to KFs, vector selection for gain turning can be applied to almost any SFA.
(ii) Various stochastic and heuristic models for estimating the unmeasurable time-varying terms in the MIMU model must be investigated. For example, applying the first- vs second-order Markov process for estimating the non-gravitational acceleration or magnetic disturbance.
(iii) Uncommon modelling techniques, such as two-layer filters or variable state KF, must be further evaluated.

## 4. Conclusion

Due to the number of publications in the field, a comprehensive survey of all publications related to SFAs for orientation tracking with MIMUs is virtually impossible. Nevertheless, in this paper, the three main strategies, including VO, CF, and KF, were surveyed and categorized, and references to more than 250 publications are provided. Specifically, for CFs and KFs, details of the filter structure, compensation strategies for correcting the raw MIMU signals, and gain tuning strategies are tabulated. Therefore, the current survey can be regarded as a source for details on the state-of-the-art SFAs, all described with a unified notation.

Moreover, we aggregated the lessons learned from the previous works to help researchers develop effective SFAs (Tables 1, 2 and 3). In summary, as shown in Fig. 3, an SFA should include the following elements: (i) offline calibration of gyroscope, accelerometer, and magnetometer; (ii) online estimation of gyroscope bias, non-gravitational

**Table 3**
Review of the state-of-the-art sensor fusion algorithms with a Kalman Filter (KF) structure, including linear KF (LKF), extended KF (EKF), and Complimentary KF (CKF). Abbreviations used in the table are described in the table footnotes.

| Study | Year | Application | Method | State vector components | Measurement-update | Notes (gain tuning or thresholding, etc.) |
|---|---|---|---|---|---|---|
| [140] | 1982 | STC | EKF | [Q, $b_G$] | [Line-of-sight attitude sensor] | - |
| [141] | 1991 | SVTC | EKF | [Velocity, $\omega$, EA, altitude, wind gust velocity] | [$y_G$, $y_M$, airspeed sensor, barometric altimeter] | - |
| [142] | 1994 | MRTC | EKF | [Attitude] | [$y_A$, gyrometric attitude] | - |
| [118] | 1995 | MRTC | LKF | [Yaw] | [$y_G$] | - |
| [153] | 1996 | HMT | CKF | [$\mathfrak{e}$ EA, $\mathfrak{e}b_G$] | [$y_G$, $y_M$] | $\mathcal{Q}\propto$ max($y_G$) $\mathcal{R}\propto$ slosh in fluid acc. |
| [157] | 1996 | MRTC | CKF | [$\mathfrak{e}$ Attitude] | [$y_A$] | - |
| [150] | 1999 | MRTC | CKF | [$\mathfrak{e}$ EA, $\mathfrak{e}b_G$] | [$y_A$, sun sensor] | - |
| [143] | 2001 | - | EKF | [Q, $\hat{\omega}$] | [$y_G$, $y_A$, $y_M$] | - |
| [143] | 2001 | - | GNA+EKF | [Q, $\hat{\omega}$] | [$\hat{q}$, $y_G$], $\hat{q}$ from GNA($y_A$, $y_M$) | - |
| [8] | 2002 | SVTC | LKF | [GPS position, GPS receiver's clock range bias, $b_G$, $b_A$] | [Position, velocity, clock] errors from the algebraic GPS equations | - |
| [119] | 2003 | - | GNA+LKF | [Q, $\hat{\omega}$] | [$\hat{q}$, $y_G$], $\hat{q}$ from GNA($y_A$, $y_M$) | - |
| [126] | 2004 | - | LKF | [Q, $\hat{\omega}$, $b_G$] | [$y_G$, $y_A$] | - |
| [28] | 2004 | HMT | LKF | [$\hat{\mathfrak{g}}$, $\hat{\mathfrak{m}}$] | [$y_A$, $y_M$] | - |
| [138] | 2004 | Walking robot motion tracking | Ensemble of two LKFs | [DCM(3)] | [$y_A$] | Switching between LKFs by $\lvert y_A\rvert$ |
| [47] | 2004 | - | LKF | [Q, $b_G$] | [$y_A$] or [$y_M$] | Adaptive $\mathcal{Q}$ |
| [54] | 2004 | HMT | CKF | [$\mathfrak{e}\hat{\mathfrak{g}}$, $\mathfrak{e}b_A$] | [$y_A$] | - |
| [210] | 2004 | - | LKF | [1D angle, $\omega$] | [1D-$y_G$] | - |
| [154] | 2004 | - | CKF | [$\mathfrak{e}$ EA, $\mathfrak{e}b_G$] | [EA from $y_A$&$y_M$] | - |
| [155] | 2004 | SVTC | CKF | [$\mathfrak{e}$ EA, $\mathfrak{e}b_G$] OR [$\mathfrak{e}$ Q, $\mathfrak{e}b_G$] | [EA from $y_A$ & $y_M$] | Switching $\mathcal{Q}$ & $\mathcal{R}$ between two levels |
| [59] | 2005 | HMT | CKF | [$\mathfrak{e}$ Helical angle/axis, $\mathfrak{e}b_G$] | [Attitude from $y_A$ & $y_G$] | - |
| [6] | 2005 | - | CKF | [$\mathfrak{e}$ Q, $\mathfrak{e}b_G$] | [Sun sensor] | - |
| [52] | 2005 | HMT | CKF | [$\mathfrak{e}$ Helical angle/axis, $\mathfrak{e}b_G$, $\mathfrak{e}\mathfrak{d}$] | [Attitude from $y_A$ & $y_G$, magnetic vector from $y_M$ & $y_G$] | - |
| [51] | 2006 | HMT | EKF | [Q, $b_A$, $b_M$] | [$y_A$, $y_M$] | Switching $\mathcal{R}$ between two levels |
| [29] | 2006 | HMT | QUEST+EKF | [Q, $\hat{\omega}$] | [$\hat{q}$, $y_G$], $\hat{q}$ from QUEST($y_A$, $y_M$) | - |
| [169] | 2006 | - | EKF | [Attitude, $\hat{\omega}$] | [$y_{A,x}$, $y_{A,y}$, $y_G$] | Adaptive acc. measurement equation |
| [131] | 2007 | - | LKF | [$\hat{\mathfrak{g}}$, $\hat{\mathfrak{m}}$] | [$y_A$, $y_M$] | Abandoning past estimations by forget factor |
| [134] | 2007 | - | LKF | EA | [EA from $y_A$ & $y_M$] | Switching $\mathcal{R}$ between two levels |
| [151] | 2007 | - | CKF | [$\mathfrak{e}$ Q, $\mathfrak{e}b_G$] | [$y_A$, $y_M$] | - |
| [158] | 2008 | AVTC | CKF | [$\mathfrak{e}$ Q] | [ $\mathfrak{e}\hat{q}$ from $y_A$ & GPS] | Tuning $\mathcal{R}$ based on $\lVert y_A - {}^{G}g \rVert$ |
| [211] | 2008 | SVTC | CKF | [$\mathfrak{e}$ Q, $\mathfrak{e}b_G$] | [$y_A$, $y_M$] | - |
| [212] | 2008 | HMT | EKF | [$\mathfrak{e}$ EA, $b_G$, $b_A$, $\mathfrak{d}$] | [$y_A$, $y_M$] | $\mathfrak{a}$ & $\mathfrak{d}$ rejection using vector selection + tuning $\mathcal{Q}$ & $\mathcal{R}$ |
| [163] | 2009 | Surgical tool motion tracking | EKF | [Q, $b_G$] | [$y_A$, $y_M$] | - |
| [122] | 2009 | HMT | LKF | [Q] | [ $\hat{q}$ from $y_A$ & $y_M$ using [123]] | $\mathfrak{a}$ & $\mathfrak{d}$ rejection using vector selection |
| [9] | 2009 | Augmented Reality | - | [EA, $\hat{\omega}$, $\hat{\dot{\omega}}$, $b_G$] | [$\hat{q}$, $y_G$], $\hat{q}$ from $y_A$ & $y_M$ | - |
| [213] | 2009 | HMT | EKF | [Velocity,$\hat{y}_A$, $\hat{\omega}$, $b_G$, Attitude] | [$y_G$, $y_A$] | - |
| [132] | 2009 | - | LKF | [$\hat{\mathfrak{g}}$, $\hat{\mathfrak{m}}$, $b_G$] | [$y_A$, $y_M$] | - |
| [55] | 2010 | - | CKF | [$\mathfrak{e}$ Q, $b_G$, $b_A$] | [$y_A$, $y_M$] | Tuning $\mathcal{R}$ using residual in acc. measurement-update |
| [164] | 2010 | HMT | EKF+Particle Filter | [EA, $b_G$] | [EA from $y_A$ & $y_M$] | - |
| [170] | 2010 | HMT | CKF | [$\mathfrak{e}$ Q] | [$y_A$, $y_M$] | Tuning $\mathcal{R}$ based on $\lVert y_A - {}^{G}g \rVert$ & $\lVert y_M - {}^{G}m \rVert$ |
| [175] | 2011 | - | CKF | [$\mathfrak{e}$ EA, $\mathfrak{e}$ velocity, $\mathfrak{e}b_G$, $\mathfrak{e}b_A$] | Velocity from GPS | $\mathcal{K}$ tuning by innovation-based adaptive estimation technique |
| [124] | 2011 | - | LKF | [Q] | [ $\hat{q}$ from FQA($y_A$, $y_M$)] | - |
| [135] | 2011 | HMT | LKF | [Q, $\mathfrak{a}$] | [$y_M$, $y_A$, $\lVert y_A \rVert$] | Switching $\mathcal{Q}$ between two levels |
| [214] | 2011 | HMT | EKF | [Q, $b_G$] | [$y_A$, $y_M$] | - |
| [215] | 2011 | HMT | CKF | [$\mathfrak{e}$ EA, $\mathfrak{e}$ position, $\mathfrak{e}$ velocity, $\mathfrak{e}b_G$, $b_A$] | [Yaw from $y_M$, $\mathfrak{e}b_G$, Velocity from ZUPT] | Heuristic heading reduction [216] |
| [147] | 2011 | HMT | EKF | [Q, $b_G$, $\mathfrak{d}$] | [$y_A$, $y_M$] | - |
| [217] | 2011 | - | EKF | [Q] | [$y_A$] | - |
| [218] | 2011 | - | CKF | [$\mathfrak{e}$ Q, $\mathfrak{e}b_G$, $\mathfrak{e}K_G$] | [$\mathfrak{e}$ EA from $y_A$ & $y_M$] | - |
| [219] | 2011 | - | EKF | [Q, $b_G$] | [$y_A$, $y_M$] | Tuning $\mathcal{R}$ based on $\lVert y_A - {}^{G}g \rVert$ |
| [220] | 2011 | - | EKF | [DCM(1), DCM(3), $b_G$] | [$y_A$, $y_M$] | - |

(continued on next page)

**Table 3** (*continued*)

| Study | Year | Application | Method | State vector components | Measurement-update | Notes (gain tuning or thresholding, etc.) |
|---|---|---|---|---|---|---|
| [221] | 2011 | HMT | CKF | [$\mathfrak{e}$ EA, $\mathfrak{e}b_G$] | [$y_M$] | Quasi-static geomagnetic field detection |
| [162] | 2012 | Surgical tool motion tracking | Two LKFs + EKF | LKF1: [$\hat{\mathfrak{g}}$], LKF2: [$\hat{\mathfrak{m}}$], EKF: [Q, $b_G$] | LKF1: [$y_A$], LKF2: [$y_M$], EKF: [ $\hat{q}$ from $y_A$ & $y_M$] | - |
| [133] | 2012 | - | LKF | [$\hat{\mathfrak{g}}$, $\hat{\mathfrak{m}}$, $b_G$] | [$y_A$, $y_M$] | - |
| [145] | 2012 | HMT | EKF | [Q, $b_G$] | [ $\hat{q}$ from $y_A$ & $y_M$] | Switching $\mathcal{R}$ a piecewise linear function |
| [222] | 2012 | HMT/ SVTC | LKF | [$\hat{\mathfrak{g}}$] | [$y_A$] | - |
| [223] | 2012 | AVTC | EKF | [DCM(3), $\hat{\omega}$, $b_G$] | [$y_A$, $y_G$] | Switching $\mathcal{R}$ between two levels |
| [224] | 2012 | HMT | LKF | [Q] | [ $\hat{q}$ from $y_A$ & $y_M$] | $\mathfrak{a}$ & $\mathfrak{d}$ rejection using vector selection |
| [148] | 2012 | - | Variable state EKF | EKF1: [Q, $b_G$, $\mathfrak{d}$]<br>EKF2: [Q, $b_G$, $\mathfrak{d}$, $\dot{\mathfrak{d}}$] | [$y_A$, $y_G$] | - |
| [225] | 2013 | - | CKF | [$\mathfrak{e}$ EA, $\mathfrak{e}b_G$, $K_G$] | [$\mathfrak{e}$ EA from $y_A$ & $y_M$] | Switching $\mathcal{R}$ between three levels |
| [166] | 2013 | - | EKF | EKF 1: [DCM(3), $\mathfrak{a}$]<br>EKF 2: [DCM(1), $\mathfrak{d}$] | EKF1: [$y_A$], EKF2: [$y_M$] | Resetting $\mathfrak{a}$ and $\mathfrak{d}$ by thresholding |
| [226] | 2013 | SVTC | CKF | [$\mathfrak{e}$ position, $\mathfrak{e}$ velocity, $\mathfrak{e}$ EA, $b_G$, $b_A$] | [Position, velocity] from GNSS | - |
| [146] | 2013 | HMT | EKF | [Q, $b_A$, $b_M$] | [$y_A$, $y_M$] | Switching $\mathcal{R}$ between two levels |
| [165] | 2013 | - | EKF | [Q] | [$y_A$, $y_M$] | - |
| [136] | 2014 | - | LKF | [Q] | [$y_A$, $y_M$] | Tuning $\mathcal{R}$ based on acc. residuals |
| [227] | 2014 | HMT | Two-layer LKF | EKF1: [$\hat{\mathfrak{g}}$], EKF2: [Yaw] | EKF1: [$y_A$], EKF2: [$y_M$] | Innovation-based adaptive estimation tuning of $\mathcal{R}$ using fuzzy logic |
| [46] | 2014 | HMT with smartphones | EKF | [Q, $b_G$, $\mathfrak{a}$] | [$y_A$, $y_M$] | - |
| [228] | 2014 | AVTC | EKF | [Q, $\hat{\omega}$, $b_G$] | [$\hat{q}$ from $y_A$ & $y_M$] | - |
| [229] | 2014 | HMT | Two-layer LKF | EKF1: [DCM(3)], EKF2: [DCM (1)] | EKF1: [$y_A$], EKF2: [$y_M$] | Switching $\mathcal{R}$ between two levels |
| [230] | 2014 | AVTC | CKF | [$\mathfrak{e}$ EA, $\mathfrak{e}b_G$, $\mathfrak{e}\mathfrak{a}$, $\mathfrak{e}\mathfrak{d}$] | [$y_A$, $y_M$] | $\mathcal{P}_A \propto Error(\mathfrak{a})$, $\mathcal{P}_M \propto Error(\mathfrak{d})$ |
| [231] | 2015 | Marine Satellite Tracking Antenna | LKF | [Q] | [$y_A$, $y_M$] | $\mathcal{Q} = \alpha \mathcal{Q}_0$, $\mathcal{R} = (1-\alpha)\mathcal{R}_0$ |
| [127] | 2015 | HMT | LKF | [$\hat{\mathfrak{g}}$, $\mathfrak{a}$] | [$y_A$] | - |
| [129] | 2015 | HMT | LKF+LKF | LKF1: [$\hat{\mathfrak{g}}$, $\mathfrak{a}$], LKF2: [$\hat{\mathfrak{m}}$, $\mathfrak{d}$] | LKF1: [$y_A$], LKF2: [$y_M$] | - |
| [232] | 2015 | AVTC | GDA+LKF | [Q] | [$y_A$] | GDA step size $\propto y_G T_s$ |
| [233] | 2015 | HMT | EKF | [Q] | [$y_A$] | Switching $\mathcal{R}$ between three levels |
| [234] | 2015 | HMT | LKF | [$\mathfrak{e}$ Yaw, $\mathfrak{e}K_G$, $b_G$] | [Yaw from $y_M$] | - |
| [161] | 2015 | HMT | LKF | [$\mathfrak{e}$ EA, $\mathfrak{e}b_G$] | - | - |
| [14] | 2015 | - | Constrained-LKF | [$\hat{\omega}$, DCM, $\mathfrak{a}$, $\mathfrak{d}$] | [$y_G$, $y_A$, $y_M$] | - |
| [15] | 2015 | - | Constrained-EKF | [DCM(3), $b_{G,\ k}$] | [$y_A$] | Tuning $\mathcal{R}$ based on $\Vert y_A \Vert$ |
| [137] | 2016 | - | LKF | [Q] | [$y_A$, $y_M$] | Tuning $\mathcal{R}$ based on accelerometer residuals |
| [235] | 2016 | AVTC | CF-EKF | [$\mathfrak{e}$ position, $\mathfrak{e}$ velocity, $\mathfrak{e}$ EA, $\mathfrak{e}b_G$, $\mathfrak{e}b_A$, $\mathfrak{e}\mathfrak{d}$] | [Position, velocity] from GNSS | - |
| [74] | 2016 | - | LKF | [Q] | [Position, velocity] from GNSS | - |
| [180] | 2016 | HMT/ SVTC | Two-layer LKF | EKF 1: [$\hat{\mathfrak{g}}$], EKF 2: [$\hat{\mathfrak{m}}$] | EKF1: [$y_A$], EKF2: [$y_M$] | Switching $\mathcal{R}$ between three levels |
| [160] | 2016 | HMT | CKF | [$\mathfrak{e}$ EA, $\mathfrak{e}b_G$] | [EA from vision system] | Adaptive fading factor by fuzzy logic |
| [236] | 2016 | HMT | LKF | [EA, $b_G$] | [Attitude from $y_A$] | $\mathcal{R} = \mathcal{R}_{nominal} + \Vert \mathfrak{a} \Vert^2$ |
| [237] | 2016 | HMT | CKF | [$\mathfrak{e}$ EA, $\mathfrak{e}b_G$] | [$y_A$, $y_M$] | Tuning $\mathcal{R}$ using Hidden Markov Model |
| [149] | 2017 | AVTC | EKF | [Q] | [$y_A$] | - |
| [238] | 2017 | SVTC | CKF | [EA, $b_G$] | [$y_A$, velocity from GPS] | - |
| [239] | 2017 | AVTC | EKF | [Q, $b_G$] | [$y_A$, $y_M$] | - |
| [125] | 2017 | AVTC | LKF | [Q] | [ $\hat{q}$ from $y_A$ & $y_M$] | - |
| [40] | 2017 | SVTC | LKF | [Q] | [$\hat{q}$ from $y_A$ & $y_M$] | $\mathfrak{d}$ rejection using vector selection |
| [130] | 2017 | - | Two-layer LKF | LKF1: [$\hat{\mathfrak{g}}$], LKF2: [$\hat{\mathfrak{m}}$] | LKF1: [$y_A$], LKF2: [$y_M$] | $\mathcal{R}_1 \propto \Vert \mathfrak{a} \Vert^2$, $\mathcal{R}_2 \propto \Vert \mathfrak{d} \Vert^2$ |
| [240] | 2017 | - | EKF | [Q, $\hat{\omega}$] | [$y_A$, $y_G$] | - |
| [241] | 2017 | Marine satellite tracking antennas | CKF | [$\mathfrak{e}$ Q, $\mathfrak{e}b_G$] | [$y_A$, $y_M$] | - |
| [242] | 2017 | Wearable robotic systems | EKF | [$EA$, $\hat{\omega}$, $\dot{\omega}$, $\dot{Q}$, $\ddot{Q}$, $d$, $d$] | [$y_G$, $y_A$, $y_M$] | - |
| [120] | 2018 | HMT with smartphones | GDA+LKF | [Q] | [$\hat{q}$], $\hat{q}$ from GDA($y_A$, $y_M$) | - |
| [172] | 2018 | - | CKF | [$\mathfrak{e}$ EA, $\mathfrak{e}b_G$] | [$y_A$, $y_G$] | Tuning $\mathcal{R}$ using Hidden Markov Model |
| [71] | 2018 | - | LKF | [Q] | [ $\hat{q}$ from $y_A$ & $y_M$] | - |
| [121] | 2018 | - | GDA+LKF | [Q] | [$\hat{q}$], $\hat{q}$ from GDA($y_A$, $y_M$) | $\mathcal{R} = \mathcal{R}_{nominal} + \alpha_k$<br>$\mathfrak{d}$ rejection using vector selection |

(*continued on next page*)

**Table 3** (*continued*)

| Study | Year | Application | Method | State vector components | Measurement-update | Notes (gain tuning or thresholding, etc.) |
|---|---|---|---|---|---|---|
| [243] | 2018 | HMT | Two-layer CKF | CKF1: [$\mathfrak{e}$ Attitude], CKF2: [$\mathfrak{e}$ Yaw] | CKF1: [ $\mathfrak{e}\widehat{q}$ from $y_A$], CKF2: [ $\mathfrak{e}\widehat{q}$ from $y_M$] | Tuning $\mathcal{R}$ by variances of errors |
| [244] | 2018 | SVTC | EKF | [Position, velocity, Q, $b_G$, $b_A$] | [Position from GPS, $\widehat{q}$ from $y_A$] | - |
| [179] | 2018 | SVTC | Two-step LKF | [Q, $b_G$] | Step1: [$y_A$, $y_{G,z}$], Step2: [$y_M$] | $\mathcal{R}_A \propto \exp(\lVert y_A - {}^G g \rVert^2)$ $\mathcal{R}_M \propto \exp(\lVert y_M - {}^G m \rVert^2)$ |
| [128] | 2019 | - | LKF+LKF | LKF1: [$\widehat{g}$], LKF2: [$\widehat{m}$] | LKF1: [$y_A$], LKF2: [$y_M$] | - |
| [245] | 2019 | HMT | CKF | [$\mathfrak{e}$ EA, $b_G$, $\mathfrak{d}$] | [$y_A$, $y_M$] | |
| [246] | 2019 | SVTC | CKF | [$\mathfrak{e}$ EA, $\mathfrak{e}$velocity, $\mathfrak{e}$position] | [Velocity, Position] from GPS | Combined Sage-Husa [247] and Strong Tracking [248] KFs |
| [249] | 2019 | HMT | EKF | [Q] | [$y_A$, $y_M$] | $\mathcal{Q} \propto cosnt + \max(\lVert \omega \rVert - thr, 0)$ $\mathcal{R}_A \propto cosnt + \max(\lvert \lVert y_A \rVert - \lVert {}^G g \rVert \rvert - thr, 0)$ $\mathcal{R}_M \propto cosnt + \max(\lvert \lVert y_M \rVert - \lVert {}^G m \rVert \rvert - thr, 0)$ |
| [250] | 2020 | HMT | EKF | [EA] | [EA] obtained by NCF | Innovation-based adaptive estimation tuning of $\mathcal{R}$ |
| [251] | 2020 | MRTC | EKF | [Q, $b_G$] | [$\widehat{q}$], $\widehat{q}$ from TRIAD($y_A$, $y_M$) | Tuning $\mathcal{R}$ by fuzzy logic |
| [252] | 2020 | HMT | LKF | [Q] | [$y_A$] | - |
| [253] | 2020 | HMT | Cascade LKF | LKF1: [DCM(3)], LKF2: [$b_G$] | LKF1: [$y_A$], LKF2: [$y_A$] | $\mathcal{R}_A \propto \lVert \mathfrak{a} \rVert^2 + \lVert y_A - {}^G g \rVert^2$ |
| [254] | 2020 | HMT | GDA+EKF | [Q, $b_G$] | [$\widehat{q}$], $\widehat{q}$ from GDA($y_A$, $y_M$) | GDA step size $\propto \lVert y_G \rVert$, $error(y_A, y_M)$ |
| [255] | 2020 | SVTC | EKF | [Q] | [$y_A$, $y_M$] | Post-EKF error reduction by proportional-integral controller |
| [256] | 2020 | AVTC | EKF | [Position, velocity, Q, $b_G$, $b_A$, LiDAR bias] | [Position, velocity, $y_A$] | - |
| [257] | 2020 | RATC | CKF | [$\mathfrak{e}$ EA, $\mathfrak{e}b_G$] | [$y_A$, $y_M$] | Adaptive tuning of $\mathcal{R}$ using ellipsoidal method |

**- Application:** STC: Spacecraft (satellite) tracking/control; HMT: Human motion tracking; MRTC: Mobile robot tracking/control; RATC: Robotic arm tracking/control; AVTC: Aerial vehicle tracking/control; SVTC: Surface vehicle tracking/control; GNSS: Global Navigation Satellite System.
**- Method:** GNA: Gauss-Newton algorithm; GDA: Gradient descent algorithm; FQA: Factored quaternion algorithm, QUEST: QUaternion ESTimator; TRIAD: TRi-axial Attitude Determination; ZUPT: Zero-Velocity-Update strategy.
**- State vector components:** Q: Quaternion parametrization of orientation; EA: Euler angle parametrization of orientation; DCM: Direction cosine matrix parametrization of orientation;. e: error of the component.
**- Measurement-update:**$b_G$: Gyroscope bias; $b_A$: Accelerometer bias; $b_M$: Magnetometer bias; $\mathfrak{a}$: external non-gravitational acceleration; $\mathfrak{d}$: magnetic disturbance;$\widehat{q}$: Orientation used in measurement-update of KF; $\widehat{\omega}$: Estimated angular velocity; $\widehat{g}$: Estimated gravitational acceleration; $\widehat{m}$: Estimated geomagnetic field.
**- Notes:**$\mathcal{Q}$: System model covariance matrix;$\mathcal{R}$: Measurement model covariance matrix; $\mathcal{P}$: State error covariance matrix; $\mathcal{K}$: Kalman filter gain.

external acceleration, and magnetic disturbance; (iii) proper implementation of the SDI as well as an algorithm for orientation estimation via the corrected accelerometer and magnetometer readouts; (iv) vector selection technique for imperfect measurement rejection; and (v) adaptive gain tuning for intelligent selection of SFA gains in real-time. Finally, the accuracy and reliability of the newly developed SFAs must be evaluated against others using a publicly available data set. This could help researchers identify the strengths and weaknesses of each SFA in practice as well as gaps to be addressed.

## Funding sources

This work was financially supported by Vanier Canada Graduate Scholarship, Alberta Innovates Graduate Student Scholarship, and Izaak Walton Killam Memorial Scholarship.

## CRediT author statement

**Milad Nazarahari:** Conceptualization, Methodology, Investigation, Writing - Original Draft, Visualization.
**Hossein Rouhani:** Conceptualization, Resources, Writing - Review & Editing, Supervision, Project administration.

## Declaration of Competing Interest

None.

## References


[1] J. Nilsson, I. Skog, Inertial sensor arrays – a literature review, in: 2016 Eur. Navig. Conf., 2016, pp. 1–10.
[2] N. Ahmad, R. Ariffin, R. Ghazilla, N.M. Khairi, Reviews on various inertial measurement unit (IMU) sensor applications, Int. J. Signal Process. Syst. 1 (2013) 256–262.
[3] M. Cornacchia, K. Ozcan, Y. Zheng, S. Velipasalar, Survey on activity detection and classification using wearable sensors, IEEE Sens. J. 17 (2017) 386–403.
[4] R. Harle, A survey of indoor inertial positioning systems for pedestrians, IEEE Commun. Surv. Tutorials. 15 (2013) 1281–1293.
[5] R. Bhardwaj, N. Kumar, V. Kumar, Errors in micro-electro-mechanical systems inertial measurement and a review on present practices of error modelling, Trans. Inst. Meas. Control. 40 (2018) 2843–2854.
[6] N.Trawny, S.I.Roumeliotis, Indirect Kalman filter for 3D attitude estimation, 2005.
[7] N.H.Q. Phuong, H.-J. Kang, Y.-S. Suh, Y.-S. Ro, A DCM based orientation estimation algorithm with an inertial measurement unit and a magnetic compass, J. Univers. Comput. Sci. 15 (2009) 859–876.
[8] H. Qi, J.B. Moore, Direct Kalman filtering approach for GPS/INS integration, IEEE Trans. Aerosp. Electron. Syst. 38 (2002) 687–693.
[9] G. Schall, D. Wagner, G. Reitmayr, E. Taichmann, M. Wieser, D. Schmalstieg, B. Hofmann-Wellenhof, Global pose estimation using multi-sensor fusion for outdoor augmented reality, in: 2009 8th IEEE Int. Symp. Mix. Augment. Real., 2009, pp. 153–162.
[10] A. Filippeschi, N. Schmitz, M. Miezal, G. Bleser, E. Ruffaldi, D. Stricker, Survey of motion tracking methods based on inertial sensors: a focus on upper limb human motion, Sensors 17 (2017).
[11] D. Choukroun, H. Weiss, I.Y. Bar-Itzhack, Y. Oshman, Direction cosine matrix estimation from vector observations using a matrix Kalman filter, IEEE Trans. Aerosp. Electron. Syst. 46 (2010) 61–79.
[12] M.D. Shuster, Constraint in attitude estimation part I: constrained estimation, J. Astronaut. Sci. 51 (2003) 51–74.
[13] I.Y. Bar-Itzhack, J. Deutschmann, F.L. Markley, Quaternion normalization in additive EKF for spacecraft attitude determination, in: Navig. Control Conf., 1991.

[14] J. Hu, K. Sun, A robust orientation estimation algorithm using MARG sensors, IEEE Trans. Instrum. Meas. 64 (2015) 815–822.
[15] H. Hyyti, A. Visala, A DCM based attitude estimation algorithm for low-cost MEMS IMUs, Int. J. Navig. Obs. Hindawi. (2015).
[16] S. Patel, H. Park, P. Bonato, L. Chan, M. Rodgers, A review of wearable sensors and systems with application in rehabilitation, J. Neuroeng. Rehabil. 9 (2012) 1–17.
[17] R. Gravina, P. Alinia, H. Ghasemzadeh, G. Fortino, Multi-sensor fusion in body sensor networks: State-of-the-art and research challenges, Inf. Fusion. 35 (2017) 68–80.
[18] M. Iosa, P. Picerno, S. Paolucci, G. Morone, Wearable inertial sensors for human movement analysis, Expert Rev. Med. Devices. 13 (2016) 641–659.
[19] G. Vannozzi, E. Bergamini, S. Fantozzi, G. Vannozzi, Trends supporting the in-field use of wearable inertial sensors for sport performance evaluation: a systematic review, Sensors 18 (2018).
[20] X. Guo, N. Ansari, F. Hu, Y. Shao, N.R. Elikplim, L. Li, A survey on fusion-based indoor positioning, IEEE Commun. Surv. Tutorials. 22 (2020) 566–594.
[21] A.M. Hasan, K. Samsudin, A.R. Ramli, R.S. Azmir, A review of navigation systems (integration and algorithms), Aust. J. Basic Appl. Sci. (2009) 943–959.
[22] Z. Yang, C. Wu, Z. Zhou, X. Zhang, X. Wang, Y. Liu, Mobility increases localizability: A survey on wireless indoor localization using inertial sensors, ACM Comput. Surv. 47 (2015) 1–34.
[23] J.L. Crassidis, F.L. Markley, Y. Cheng, A survey of nonlinear attitude estimation methods, J. Guid. Control. Dyn. 30 (2007).
[24] A. Cavallo, A. Cirillo, P. Cirillo, G. De Maria, P. Falco, C. Natale, S. Pirozzi, Experimental comparison of sensor fusion algorithms for attitude estimation, IFAC, 2014.
[25] S.O.H. Madgwick, A.J.L. Harrison, R. Vaidyanathan, Estimation of IMU and MARG orientation using a gradient descent algorithm, in: 2011 IEEE Int. Conf. Rehabil. Robot., Zurich, 2011, pp. 1–7.
[26] R. Mahony, T. Hamel, J.-M. Pflimlin, Non-linear complementary filters on the special orthogonal group, IEEE Trans. Automat. Contr. 53 (2008) 1203–1218.
[27] M. Gietzelt, K.H. Wolf, M. Marschollek, R. Haux, Performance comparison of accelerometer calibration algorithms based on 3D-ellipsoid fitting methods, Comput. Methods Programs Biomed. 111 (2013) 62–71.
[28] R. Zhu, Z. Zhou, A real-time articulated human motion tracking using tri-axis inertial/magnetic sensors package, IEEE Trans. Neural Syst. Rehabil. 12 (2004) 295–302.
[29] X. Yun, E.R. Bachmann, Design, implementation and experimental results of a quaternion-based Kalman filter for human body motion tracking, IEEE Trans. Robot. 22 (2006) 1216–1227.
[30] A.D. Young, Use of body model constraints to improve accuracy of inertial motion capture, in: 2010 Int. Conf. Body Sens. Networks, BSN 2010, 2010, pp. 180–186.
[31] G. Bleser, G. Hendeby, M. Miezal, Using egocentric vision to achieve robust inertial body tracking under magnetic disturbances, in: Proc. 2011 10th IEEE Int. Symp. Mix. Augment. Real., 2011, pp. 103–109.
[32] L. Peppoloni, A. Filippeschi, E. Ruffaldi, C.A. Avizzano, A novel 7 degrees of freedom model for upper limb kinematic reconstruction based on wearable sensors, in: Proc. 2013 IEEE 11th Int. Symp. Intell. Syst. Informatics, 2013, pp. 105–110.
[33] A.D. Young, Comparison of orientation filter algorithms for realtime wireless inertial posture tracking, in: Proc. - 2009 6th Int. Work. Wearable Implant. Body Sens. Networks, BSN 2009, 2009, pp. 59–64.
[34] M.D. Shuster, S.D. Oh, Three-axis attitude determination from vector observations, J. Guid. Control. Dyn. 4 (1981) 70–77.
[35] G. Lerner, Spacecraft attitude determination and control. Spacecr. Attitude Determ. Control, Kluwer Academic, 1978, pp. 420–428.
[36] X. Yun, E. Bachmann, R. McGhee, A simplified quaternion based algorithm for orientation estimation from Earth gravity and magnetic field measurements, IEEE Trans. Instrum. Meas. 57 (2008) 638–650.
[37] A.M. Sabatini, Estimating three-dimensional orientation of human body parts by inertial/magnetic sensing, Sensors 11 (2011) 1489–1525.
[38] B. Fan, Q. Li, T. Liu, How magnetic disturbance influences the attitude and heading in magnetic and inertial sensor-based orientation estimation, Sensors (Switzerland) 18 (2018).
[39] G. Ligorio, A.M. Sabatini, Dealing with magnetic disturbances in human motion capture: A survey of techniques, Micromachines 7 (2016).
[40] K. Feng, J. Li, X. Zhang, C. Shen, Y. Bi, T. Zheng, J. Liu, A new quaternion-based kalman filter for real-time attitude estimation using the two-step geometrically-intuitive correction algorithm, Sensors 17 (2017).
[41] S. Madgwick, AHRS Algorithms and Calibration Solutions to Facilitate New Applications Using Low-Cost MEMS, University of Bristol, 2014.
[42] E. Bergamini, G. Ligorio, A. Summa, G. Vannozzi, A. Cappozzo, A.M. Sabatini, Estimating orientation using magnetic and inertial sensors and different sensor fusion approaches: accuracy assessment in manual and locomotion tasks, Sensors (2014) 18625–18649.
[43] M. Caruso, A.M. Sabatini, M. Knaflitz, M. Gazzoni, U. Della Croce, A. Cereatti, Accuracy of the orientation estimate obtained using four sensor fusion filters applied to recordings of magneto-inertial sensors moving at three rotation rates, in: 2019 41st Annu. Int. Conf. IEEE Eng. Med. Biol. Soc., 2019.
[44] Open Source Sensor Fusion, (n.d.). https://github.com/memsindustrygroup/Open-Source-Sensor-Fusion/tree/master/docs.
[45] T. Michel, H. Fourati, P. Genev, N. Laya, A comparative analysis of attitude estimation for pedestrian navigation with smartphones, in: Nternational Conf. Indoor Position. Indoor Navig, 2015.
[46] V. Renaudin, C. Combettes, Magnetic, acceleration fields and gyroscope quaternion (MAGYQ)-based attitude estimation with smartphone sensors for indoor pedestrian navigation, Sensors 14 (2014) 22864–22890.
[47] D. Choukroun, I.Y. Bar-Itzhack, Y. Oshman, Novel quaternion Kalman filter, EEE Trans. Aerosp. Electron. Syst. 14 (2004) 20008–20024.
[48] H. Fourati, Heterogeneous data fusion algorithm for pedestrian navigation via foot-mounted inertial measurement unit and complementary filter, IEEE Trans. Instrum. Meas. 64 (2015) 221–229.
[49] P. Martin, E. Salaun, Design and implementation of a low-cost observer-based attitude and heading reference system, Control Eng. Pract. 18 (2010) 712–722.
[50] M. Carratu, S. Dello Iacono, M.Long Hoang, A. Pietrosanto, Energy characterization of attitude algorithms, in: IEEE Int. Conf. Ind. Informatics, 2019, pp. 1585–1590.
[51] Angelo M. Sabatini, Quaternion-based extended Kalman filter for determining orientation by inertial and magnetic sensing, IEEE Trans. Biomed. Eng. 53 (2006) 1346–1356.
[52] D. Roetenberg, H.J. Luinge, C.T.M. Baten, P.H. Veltink, Compensation of magnetic disturbances improves inertial and magnetic sensing of human body segment orientation, IEEE Trans. Neural Syst. Rehabil. Eng. 13 (2005) 395–405.
[53] F. Ferraris, U. Grimaldi, M. Parvis, Procedure for effortless in-field calibration of three-axis rate gyros and accelerometers, Sensors Mater 7 (1995) 311–330.
[54] H.J. Luinge, P.H. Veltink, Inclination measurement of human movement using a 3-D accelerometer with autocalibration, IEEE Trans. Neural Syst. Rehabil. Eng. 12 (2004) 112–121.
[55] Y.S. Suh, Orientation estimation using a quaternion-based indirect kalman filter with adaptive estimation of external acceleration, IEEE Trans. Instrum. Meas. 59 (2010) 3296–3305.
[56] J.C.K. Chou, Quaternion kinematic and dynamic differential equations, IEEE Trans. Robot. Autom. 8 (1992) 53–64.
[57] J.K. Lee, M.J. Choi, Effect of strapdown integration order and sampling rate on IMU-based attitude estimation accuracy, Sensors (Switzerland) 18 (2018).
[58] Y. Hao, Z. Xiong, W. Gao, L. Li, Study of strapdown inertial navigation integration algorithms, in: Proc. 2004 Int. Conf. Intell. Mechatronics Autom., 2004, pp. 751–754, https://doi.org/10.1109/icima.2004.1384296.
[59] H.J. Luinge, P.H. Veltink, Measuring orientation of human body segments using miniature gyroscopes and accelerometers, Med. Biol. Eng. Comput. 43 (2005) 273–282.
[60] I. Pasciuto, G. Ligorio, E. Bergamini, G. Vannozzi, A.M. Sabatini, A. Cappozzo, How angular velocity features and different gyroscope noise types interact and determine orientation estimation accuracy, Sensors (Switzerland) 15 (2015) 23983–24001.
[61] G. Wahba, A least squares estimate of spacecraft attitude, SIAM Rev 7 (1965) 409.
[62] F.L.Markley, D.Mortari, How to estimate attitude from vector observations, (1999).
[63] I.Y. Bar-Itzhack, R.R. Harman, Optimized TRIAD algorithm for attitude determination, J. Guid. Control. Dyn. 20 (1997) 208–211.
[64] M.D. Shuster, S.D. Oh, Three-axis attitude determination from vector observations, J. Guid. Control. Dyn. 4 (1981) 70–77.
[65] P.B. Davenport, A vector approach to the algebra of rotations with applications, NASA, Tech. Rep. (1968).
[66] F.L. Markley, Attitude determination from vector observations: A fast optimal matrix algorithm, J. Astronaut. Sci. 41 (1993) 261–280.
[67] F.L. Markley, Attitude determination using vector observations and the singular value decomposition, J. Astronaut. Sci. 36 (1988) 245–258.
[68] M.D. Shuster, Filter QUEST or REQUEST, J. Guid. Control. Dyn. 32 (2009) 643–645.
[69] I.Y. Bar-Itzhack, REQUEST—A recursive QUEST algorithm for sequential attitude determination, J. Guid. Control. Dyn. 19 (1996) 1034–1038.
[70] J. Wu, Z. Zhou, B. Gao, R. Li, Y. Cheng, H. Fourati, Fast linear quaternion attitude estimator using vector observations, IEEE Trans. Autom. Sci. Eng. 15 (2018) 307–319.
[71] J. Wu, Z. Zhou, H. Fourati, M. Liu, Recursive linear continuous quaternion attitude estimator from vector observations, IET Radar, Sonar Navig 12 (2018) 1196–1207.
[72] D. Gebre-Egziabher, G.H. Elkaim, J. Powell, B.W. Parkinson, A gyro-free quaternion-based attitude determination system suitable for implementation using low cost sensors, in: 2000 IEEE Position Locat. Navig. Symp., San Diego, CA, USA, 2000, pp. 185–192.
[73] R.G. Valenti, I. Dryanovski, J. Xiao, Keeping a good attitude: A quaternion-based orientation filter for IMUs and MARGs, Sensors 15 (2015) 19302–19330.
[74] R.G. Valenti, I. Dryanovski, J. Xiao, A linear Kalman filter for MARG orientation estimation using the algebraic quaternion algorithm, IEEE Trans. Instrum. Meas. 65 (2016) 467–481.
[75] J. Calusdian, X. Yun, E. Bachmann, Adaptive-gain complementary filter of inertial and magnetic data for orientation estimation, Proc. - IEEE Int. Conf. Robot. Autom. (2011) 1916–1922.
[76] E.R. Bachmann, I. Duman, U.Y. Usta, R.B. McGhee, X.P. Yun, M.J. Zyda, Orientation tracking for humans and robots using inertial sensors, in: Proc. 1999 IEEE Int. Symp. Comput. Intell. Robot. Autom. CIRA'99 (Cat. No.99EX375), 1999, pp. 187–194.
[77] J.K. Lee, E.J. Park, A fast quaternion-based orientation optimizer via virtual rotation for human motion tracking, IEEE Trans. Biomed. Eng. 56 (2009) 1574–1582.
[78] H. Fourati, N. Manamanni, L. Afilal, Y. Handrich, A nonlinear filtering approach for the attitude and dynamic body acceleration estimation based on inertial and magnetic sensors: bio-logging application, IEEE Sens. J. 11 (2011) 233–244.

[79] H. Fourati, N. Manamanni, L. Afilal, Y. Handrich, Complementary observer for body segments motion capturing by inertial and magnetic sensors, IEEE/ASME Trans. Mechatronics. 19 (2014) 149–157.
[80] Y. Tian, H.X. Wei, J.D. Tan, An adaptive-gain Complementary Filter for real-time human motion tracking with MARG sensors in free-living environments, IEEE Trans. Neural Syst. Rehabil. Eng. 21 (2013) 254–264.
[81] M.B. Del Rosario, N.H. Lovell, S.J. Redmond, Quaternion-based complementary filter for attitude determination of a smartphone, IEEE Sens. J. 16 (2016) 6008–6017.
[82] B. Fan, Q. Li, C. Wang, T. Liu, An adaptive orientation estimation method for magnetic and inertial sensors in the presence of magnetic disturbances, Sensors (Switzerland) (2017) 17.
[83] J. Wu, Z. Zhou, H. Fourati, R. Li, M. Liu, Generalized linear quaternion complementary filter for attitude estimation from multisensor observations: an optimization approach, IEEE Trans. Autom. Sci. Eng. 16 (2019) 1330–1343.
[84] S. Ghasemi-Moghadam, M.R. Homaeinezhad, Attitude determination by combining arrays of MEMS accelerometers, gyros, and magnetometers via quaternion-based complementary filter, Int. J. Numer. Model. Electron. Networks, Devices Fields. 31 (2018) 1–24.
[85] C. Yi, J. Ma, H. Guo, J. Han, H. Gao, F. Jiang, C. Yang, Estimating three-dimensional body orientation based on an improved complementary filter for human motion tracking, Sensors 18 (2018) 1–19.
[86] Y. Guan, X. Song, Sensor fusion of gyroscope and accelerometer for low-cost attitude determination system, in: Proc. 2018 Chinese Autom. Congr. CAC 2018, IEEE, 2018, pp. 1068–1072.
[87] R. Zhu, Z. Zhou, A small low-cost hybrid orientation system and its error analysis, IEEE Sens. J. 9 (2009) 223–230.
[88] P. Daponte, L. De Vito, S. Rapuano, M. Riccio, F. Picariello, Compensating magnetic disturbances on MARG units by means of a low complexity data fusion algorithm, in: Proc. 2015 IEEE Int. Symp. Med. Meas. Appl. MeMeA 2015, IEEE, 2015, pp. 157–162.
[89] J. Cockcroft, J.H. Muller, C. Scheffer, A complementary filter for tracking bicycle crank angles using inertial sensors, kinematic constraints, and vertical acceleration updates, IEEE Sens. J. 15 (2015) 4218–4225.
[90] M. Kok, T.B. Schön, A fast and robust algorithm for orientation estimation using inertial sensors, IEEE Signal Process. Lett. 26 (2019) 1673–1677.
[91] Y.C. Lai, S.S. Jan, F. Bin Hsiao, Development of a low-cost attitude and heading reference system using a three-axis rotating platform, Sensors 10 (2010) 2472–2491.
[92] R. Chang, X. Mu, X. Shen, Attitude estimation with complementary filter, Appl. Mech. Mater. 44–47 (2011) 3781–3784.
[93] T.S. Yoo, S.K. Hong, H.M. Yoon, S. Park, Gain-scheduled complementary filter design for a MEMS based attitude and heading reference system, Sensors 11 (2011) 3816–3830.
[94] M. Euston, P. Coote, R. Mahony, J. Kim, T. Hamel, A complementary filter for attitude estimation of a fixed-wing UAV, in: Proceeding 2008 IEEE Int. Conf. Intell. Robot. Syst., 2008, pp. 340–345.
[95] X. Wen, C. Liu, Z. Huang, S. Su, X. Guo, Z. Zuo, H. Qu, A first-order differential data processing method for accuracy improvement of complementary filtering in micro-UAV attitude estimation, Sensors (Switzerland) 19 (2019).
[96] A. Khosravian, M. Namvar, Rigid body attitude control using a single vector measurement and gyro, IEEE Trans. Automat. Contr. 57 (2012) 1273–1279.
[97] Y. Wang, E. Chang-Siu, M. Brown, M. Tomizuka, M.I. Almajed, B.N. Alsuwaidan, Three dimensional attitude estimation via the triad algorithm and a time-varying complementary filter, in: 5th Annu. Dyn. Syst. Control Conf. Jt. with JSME 2012 11th Motion Vib. Conf., 2012, pp. 157–165.
[98] R.B. Widodo, H. Edayoshi, C. Wada, Complementary filter for orientation estimation: Adaptive gain based on dynamic acceleration and its change, in: 2014 Jt. 7th Int. Conf. Soft Comput. Intell. Syst. SCIS 2014 15th Int. Symp. Adv. Intell. Syst. ISIS 2014, IEEE, 2014, pp. 906–909.
[99] H.F. Grip, T.I. Fossen, T.A. Johansen, A. Saberi, Attitude estimation based on time-varying reference vectors with biased gyro and vector measurements, IEEE Trans. Automat. Contr. 44 (2011) 8497–8502.
[100] K.J. Jensen, Generalized nonlinear complementary attitude filter, J. Guid. Control. Dyn. 34 (2011) 1588–1592.
[101] O. De Silva, G.K.I. Mann, R.G. Gosine, The right invariant nonlinear complementary filter for low cost attitude and heading estimation of platforms, J. Dyn. Syst. Meas. Control. Trans. ASME. (2018) 140.
[102] M.D. Hua, G. Ducard, T. Hamel, R. Mahony, K. Rudin, Implementation of a nonlinear attitude estimator for aerial robotic vehicles, IEEE Trans. Control Syst. Technol. 22 (2014) 201–213.
[103] B. Fan, Q. Li, T. Liu, Improving the accuracy of wearable sensor orientation using a two-step complementary filter with state machine-based adaptive strategy, Meas. Sci. Technol. 29 (2018).
[104] J. Wu, Z. Zhou, J. Chen, H. Fourati, R. Li, Fast complementary filter for attitude estimation using low-cost MARG sensors, IEEE Sens. J. 16 (2016) 6997–7007.
[105] P. Marantos, Y. Koveos, K.J. Kyriakopoulos, UAV state estimation using adaptive complementary filters, IEEE Trans. Control Syst. Technol. 24 (2016) 1214–1226.
[106] Q.Q. Yang, L.L. Sun, L. Yang, A fast adaptive-gain complementary filter algorithm for attitude estimation of an unmanned aerial vehicle, J. Navig. 71 (2018) 1478–1491.
[107] J. Chang, J. Cieslak, A. Zolghadri, J. Dávila, J. Zhou, Design of sliding mode observers for quadrotor pitch/roll angle estimation via IMU measurements, in: 2015 Work. Res. Educ. Dev. Unmanned Aer. Syst. RED-UAS 2015, 2016, pp. 393–400.
[108] J. Chang, J. Cieslak, J. Dávila, J. Zhou, A. Zolghadri, Z. Guo, A two-step approach for an enhanced quadrotor attitude estimation via IMU data, IEEE Trans. Control Syst. Technol. 26 (2018) 1140–1148.
[109] A.El Hadri, A. Benallegue, Sliding mode observer to estimate both the attitude and the gyro-bias by using low-cost sensors, in: 2009 IEEE/RSJ Int. Conf. Intell. Robot. Syst., 2009.
[110] J.F. Vasconcelos, B. Cardeira, C. Silvestre, P. Oliveira, P. Batista, Discrete-time complementary filters for attitude and position estimation: design, analysis and experimental validation, IEEE Trans. Control Syst. Technol. 19 (2011) 181–198, https://doi.org/10.1016/j.ifacol.2019.11.274.
[111] A. Tayebi, S. McGilvray, A. Roberts, M. Moallem, Attitude estimation and stabilization of a rigid body using low-cost sensors, in: Proc. IEEE Conf. Decis. Control, 2007, pp. 6424–6429.
[112] H. Sheng, T. Zhang, MEMS-based low-cost strap-down AHRS research, Meas. J. Int. Meas. Confed. 59 (2015) 63–72.
[113] Z. Wu, Z. Sun, W. Zhang, Q. Chen, A novel approach for attitude estimation based on MEMS inertial sensors using nonlinear complementary filters, IEEE Sens. J. 16 (2016) 3856–3864.
[114] A.A. Neto, D.G. Macharet, V.C. da Silva Campos, M.F.M. Campos, Adaptive complementary filtering algorithm for mobile robot localization, J. Brazilian Comput. Soc. 15 (2009) 19–31.
[115] R. Kottath, P. Narkhede, V. Kumar, V. Karar, S. Poddar, Multiple model adaptive complementary filter for attitude estimation, Aerosp. Sci. Technol. 69 (2017) 574–581.
[116] S. Poddar, P. Narkhede, V. Kumar, A. Kumar, PSO aided adaptive complementary filter for attitude estimation, J. Intell. Robot. Syst. Theory Appl. 87 (2017) 531–543.
[117] Dan Simon, Optimal State Estimation, Kalman, H-infinity, and Nonlinear Approaches, John Wiley & Sons, Inc., 2006.
[118] B. Barshan, H.F. Durrant-whyte, Evaluation of a solid-state gyroscope for robotics applications, IEEE Trans. Instrum. Meas. 44 (1995) 61–67.
[119] X. Yun, M. Lizarraga, E.R. Bachmann, R.B. McGhee, An improved quaternion-based kalman filter for real-time tracking of rigid body orientation, in: Proc. 2003 IEEWRSJ Inll. Conf. Intell. Robot. Syst., 2003, pp. 1074–1079.
[120] S. Yean, B.S. Lee, C.K. Yeo, C.H. Vun, H.L. Oh, Smartphone orientation estimation algorithm combining kalman filter with gradient descent, IEEE J. Biomed. Heal. Informatics. 22 (2018) 1421–1433.
[121] L. Wöhle, M. Gebhard, A robust quaternion based kalman filter using a gradient descent algorithm for orientation measurement, in: Proc. 2018 IEEE Int. Instrum. Meas. Technol. Conf., 2018.
[122] J.K. Lee, E.J. Park, Minimum-order kalman filter with vector selector for accurate estimation of human body orientation, IEEE Trans. Robot. 25 (2009) 1196–1201.
[123] F.L. Markley, Fast quaternion attitude estimation from two vector measurements, J. Guid. Control. Dyn. 25 (2002) 411–414.
[124] E. Seo, C. Park, D. Kim, J. Song, Quaternion-based orientation estimation with static error reduction, in: Proc. 2011 IEEE Int. Conf. Mechatronics Autom., IEEE, 2011, pp. 1624–1629.
[125] S. Guo, J. Wu, Z. Wang, J. Qian, Novel MARG-sensor orientation estimation algorithm using Fast Kalman Filter, J. Sensors. (2017) 1–12.
[126] A. Kim, M.F. Golnaraghi, A quaternion-based orientation estimation algorithm using an inertial measurement unit, in: Rec. - IEEE PLANS, Position Locat. Navig. Symp., 2004, pp. 268–272.
[127] G. Ligorio, A.M. Sabatini, A novel kalman filter for human motion tracking with an inertial-based dynamic inclinometer, IEEE Trans. Biomed. Eng. 62 (2015) 2033–2043.
[128] J.K. Lee, A parallel attitude-heading kalman filter without state-augmentation of model-based disturbance components, IEEE Trans. Instrum. Meas. 68 (2019) 2668–2670.
[129] G. Ligorio, A.M. Sabatini, A linear kalman filtering-based approach for 3D orientation estimation from magnetic/inertial sensors, in: Proc. 2015 IEEE Int. Conf. Multisens. Fusion Integr. Intell. Syst., IEEE, 2015, pp. 77–82.
[130] J.K. Lee, M.J. Choi, A sequential orientation kalman filter for AHRS limiting effects of magnetic disturbance to heading estimation, J. Electr. Eng. Technol. 12 (2017) 1921–1928.
[131] R. Zhu, D. Sun, Z. Zhou, D. Wang, A linear fusion algorithm for attitude determination using low cost MEMS-based sensors, Measurement 40 (2007) 322–328.
[132] P. Batista, C. Silvestre, P. Oliveira, Sensor-based complementary globally asymptotically stable filters for attitude estimation, in: Jt. 48th IEEE Conf. Decis. Control 28th Chinese Control Conf., 2009, pp. 7563–7568.
[133] P. Batista, C. Silvestre, P. Oliveira, S. Member, Sensor-based globally asymptotically stable filters for attitude estimation: analysis, design, and performance evaluation, IEEE Trans. Automat. Contr. 57 (2012) 2095–2100.
[134] D. Jurman, M. Jankovec, R. Kamnik, M. Topic, Calibration and data fusion solution for the miniature attitude and heading reference system, Sensors Actuators A 138 (2007) 411–420.
[135] S. Sun, X. Meng, L. Ji, Z. Huang, J. Wu, Adaptive kalman filter for orientation estimation in micro-sensor motion capture, in: Proceeding 14th Int. Conf. Inf. Fusion, 2011.
[136] A. Makni, H. Fourati, A.Y. Kibangou, Adaptive kalman filter for MEMS-IMU based attitude estimation under external acceleration and parsimonious use of gyroscopes, in: Proc. 2014 Eur. Control Conf., EUCA, 2014, pp. 1379–1384.
[137] A. Makni, H. Fourati, A.Y. Kibangou, A. Makni, H. Fourati, A.Y. Kibangou, E. A. Attitude, A. Makni, H. Fourati, A.Y. Kibangou, Energy-aware adaptive attitude estimation under external acceleration for pedestrian navigation, IEEE Trans. Instrum. Meas. 21 (2016) 1366–1375.

[138] H. Rehbinder, X. Hu, Drift-free attitude estimation for accelerated rigid bodies, Automatica 40 (2004) 653–659.
[139] H. Rehbinder, X. Hu, Nonlinear pitch and roll estimation for walking robots, in: Proc. IEEE Int. Conf. Robot. Autom, 2000, pp. 2617–2622.
[140] E.J. Lefferts, F.L. Markley, M.D. Shuster, Kalman filtering for spacecraft attitude estimation, J. Guid. Control. Dyn. 4 (1982) 417–429.
[141] M. Koifman, S.J. Merhav, Autonomously aided strapdown attitude reference system, J. Guid. Control. Dyn. 14 (1991) 1164–1172.
[142] J. Vaganay, M.J. Aldon, Attitude estimation for a vehicle using inertial sensors, Control Eng. Pract. 2 (1994) 281–287.
[143] J.L. Marins, X. Yun, E.R. Bachmann, R.B. Mcghee, M.J. Zyda, An extended kalman filter for quaternion-based orientation estimation using, in: Proceeding 2001 IEEE/RSJ Int. Conf. Intell. Robot. Syst., 2001, pp. 2003–2011.
[144] X. Yun, C. Aparicio, E.R. Bachmann, R.B. McGhee, Implementation and experimental results of a quaternion-based kalman filter for human body motion tracking, in: Proc. 2005 IEEE Int. Conf. Robot. Autom., 2005, pp. 317–322.
[145] C. Mazzà, M. Donati, J. McCamley, P. Picerno, A. Cappozzo, An optimized Kalman filter for the estimate of trunk orientation from inertial sensors data during treadmill walking, Gait Posture 35 (2012) 138–142.
[146] S. Zhang, K. Xiao, Q. Zhang, H. Zhang, Y. Liu, Improved extended kalman fusion method for upper limb motion estimation with inertial sensors, in: Proc. Fourth Int. Conf. Intell. Control Inf. Process, 2013, pp. 587–593.
[147] A.M. Sabatini, Kalman-filter-based orientation determination using inertial/magnetic sensors: Observability analysis and performance evaluation, Sensors 11 (2011) 9182–9206.
[148] A.M. Sabatini, Variable-state-dimension Kalman-based filter for orientation determination using inertial and magnetic sensors, Sensors 12 (2012) 8491–8506.
[149] Y. Xu, J. Guo, Y. Guan, EKF based multiple-mode attitude estimator for quadrotor using inertial measurement unit, in: Proc. 36th Chinese Control Conf, 2017, pp. 6191–6198.
[150] S.I. Roumeliotis, G.S. Sukhatme, G.A. Bekey, Smoother based 3D attitude estimation for mobile robot localization, Proc. IEEE Int. Conf. Robot. Autom. 3 (1999) 1979–1986.
[151] M. Ahmadi, A. Khayatian, P. Karimaghaee, Orientation estimation by error-state extended kalman filter in quaternion vector space, in: SICE Annu. Conf. 2007, 2007, pp. 60–67.
[152] R.G. Brown, P.Y.C. Hwang, Introduction to Random Signals and Applied Kalman Filtering, 2nd edn., John Wiley & Sons, Inc., New York, 1992.
[153] E. Foxlin, Inertial head-tracker sensor fusion by a complementary separate-bias Kalman filter, in: Proc. IEEE 1996 Virtual Real. Annu. Int. Symp., 1996, pp. 185–194.
[154] P. Setoodeh, A. Khayatian, E. Farjah, Attitude estimation by separate-bias kalman filter-based data fusion, J. Navig. 57 (2004) 261–273.
[155] D. Gebre-egziabher, R.C. Hayward, J.D. Powell, Design of multi-sensor attitude determination systems, IEEE Trans. Aerosp. Electron. Syst. 40 (2004) 627–649.
[156] R. Zhang, L.M. Reindl, Pedestrian motion based inertial sensor fusion by a modified complementary separate-bias kalman filter, in: Proc. 2011 IEEE Sensors Appl. Symp., IEEE, 2011.
[157] Y. Fuke, E. Krotkov, Dead reckoning for a lunar rover on uneven terrain, in: Proc. 1996 IEEE Inertnational Conf. Robot. Autom., 1996, pp. 411–416.
[158] J.K. Hall, N.B. Knoebel, T.W. McLain, Quaternion attitude estimation for miniature air vehicles using a multiplicative extended kalman filter, in: 2008 IEEE/ION Position, Locat. Navig. Symp., 2008, pp. 1230–1237.
[159] G.F. Welch, SCAAT: Incremental Tracking with Incomplete Information, University of North Carolina at Chapel Hill, 1996.
[160] C.H. Kang, C.G. Park, J.W. Song, An adaptive complementary kalman filter using fuzzy logic for a hybrid head tracker system, IEEE Trans. Instrum. Meas. 65 (2016) 2163–2173.
[161] R. Kannan, Orientation estimation based on LKF using differential state equation, IEEE Sens. J. 15 (2015) 6156–6163.
[162] H. Ren, P. Kazanzides, Investigation of attitude tracking using an integrated inertial and magnetic navigation system for hand-held surgical instruments, IEEE Trans. Mechatronics. 17 (2012) 210–217.
[163] H. Ren, P. Kazanzides, Hybrid attitude estimation for laparoscopic surgical tools: a preliminary study, in: 31st Annu. Int. Conf. IEEE EMBS, 2009, pp. 5583–5586.
[164] J. Musić, M. Cecić, V. Zanchi, Real-time body orientation estimation based on two-layer stochastic filter architecture, Automatika 51 (2010) 264–274.
[165] S. Sabatelli, M. Galgani, L. Fanucci, A. Rocchi, A double-stage kalman filter for orientation tracking with an integrated processor in 9-D IMU, IEEE Trans. Instrum. Meas. 62 (2013) 590–598.
[166] A. Dang, V. Nguyen, DCM-based orientation estimation using cascade of two adaptive extended Kalman filters, in: Proceeding 2013 Int. Conf. Control. Autom. Inf. Sci., IEEE, 2013, pp. 152–157.
[167] C. Hide, T. Moore, M. Smith, Adaptive kalman filtering for low-cost INS/GPS, J. Navig. 56 (2003) 143–152.
[168] C. Hu, Y. Chen, W. Chen, Adaptive Kalman filtering for DGPS positioning, in: Int. Symp. Kinematic Syst. Geod. Geomatics Navig., 2001.
[169] Y.-S. Shu, S.-K. Park, H.-J. Kank, Y.-S. Ro, Attitude estimation adaptively compensating external acceleration, JSME Int. J. Ser. C Mech. Syst. Mach. Elem. Manuf. 49 (2006) 172–179.
[170] S. Sun, X. Meng, L. Ji, J. Wu, W.-C. Wong, Adaptive sensor data fusion in motion capture, in: Proc. 13th Int. Conf. Inf. Fusion, IEEE, 2010.
[171] M.E. Johnson, T. Sathyan, Improved orientation estimation in complex environments using low-cost inertial sensors, in: 14th Int. Conf. Inf. Fusion, IEEE, 2011.
[172] X. Tong, Z. Li, G. Han, N. Liu, Y. Su, J. Ning, F. Yang, Adaptive EKF based on HMM recognizer for attitude estimation using MEMS MARG sensors, IEEE Sens. J. 18 (2018) 3299–3310.
[173] F. Jamil, N. Iqbal, S. Ahmad, D.H. Kim, Toward accurate position estimation using learning to prediction algorithm in indoor navigation, Sensors (Switzerland) 20 (2020) 1–27.
[174] R. Mehra, Approaches to adaptive filtering, IEEE Trans. Automat. Contr. 17 (1972) 693–698.
[175] F. Jiancheng, Y. Sheng, Study on innovation adaptive EKF for in-flight alignment of airborne POS, IEEE Trans. Instrum. Meas. 60 (2011) 1378–1388.
[176] P.D. Hanlon, P.S. Maybeck, Multiple-model adaptive estimation using a residual correlation Kalman filter bank, IEEE Trans. Aerosp. Electron. Syst. 36 (2000) 393–406.
[177] J. Li, K. Shu, H. Zhang, An efficient method for tri-axis magnetometer calibration, in: IEEE SmartWorld, Ubiquitous Intell. Comput. Adv. Trust. Comput. Scalable Comput. Commun. Internet People Smart City Innov. SmartWorld/UIC/ATC/SCALCOM/IOP/SCI 2019, IEEE, 2019, pp. 654–660.
[178] D. Gebre-Egziabher, G. Elkaim, J. Powell, B. Parkinson, A non-linear, two-step estimation algorithm for calibrating solid-state strapdown magnetometers, in: 8th Int. Conf. Integr. Navig. Syst., 2001, pp. 290–297.
[179] G. Shi, X. Li, Z. Jiang, An improved yaw estimation algorithm for land vehicles using MARG sensors, Sensors 18 (2018).
[180] S. Zhang, S. Yu, C. Liu, X. Yuan, S. Liu, A dual-linear kalman filter for real-time orientation determination system using low-cost MEMS sensors, Sensors 16 (2016).
[181] M. Carratù, S. Dello Iacono, M. Ferro, V. Paciello, A. Pietrosanto, Test platform for data fusion application in indoor positioning. Sensors Microsystems, AISEM 2019, Lect. Notes Electr. Eng, Springer International Publishing, 2020, pp. 329–333.
[182] R. Bischoff, U. Huggenberger, E. Prassler, KUKA youBot - A mobile manipulator for research and education, in: Proc. - IEEE Int. Conf. Robot. Autom., 2011, pp. 1–4.
[183] F. Alam, Z. Zhaihe, H. Jiajia, A comparative analysis of orientation estimation filters using MEMS based IMU, 2nd Int. Conf. Res. Sci. Eng. Technol. (2014).
[184] T. Hamel, R. Mahony, Attitude estimation on SO(3) based on direct inertial measurements, in: Proc. 2006 IEEE Int. Conf. Robot. Autom. ICRA, 2006, p. 2006.
[185] S.A. Ludwig, K.D. Burnham, Comparison of Euler estimate using extended kalman filter, madgwick and mahony on quadcopter flight data, in: 2018 Int. Conf. Unmanned Aircr. Syst., 2018, pp. 1236–1241.
[186] G.H. Lee, M. Achtelik, F. Fraundorfer, M. Pollefeys, R. Siegwart, A benchmarking tool for MAV visual pose estimation, in: 2010 11th Int. Conf. Control Autom. Robot. Vis., 2010.
[187] X. Li, Y. Wang, Evaluation of AHRS algorithms for foot-mounted inertial-based indoor navigation systems, GeoScape 11 (2019) 48–63.
[188] M. Angermann, P. Robertson, T. Kemptner, M. Khider, A high precision reference data set for pedestrian navigation using foot-mounted inertial sensors, in: Int. Conf. Indoor Position. Indoor Navig, 2010, pp. 1–6.
[189] J. Tosi, F. Taffoni, A. Hussain, D. Campolo, D. Formica, Methodology for the evaluation of magneto-inertial orientation filters in SO(3), in: 2019 II Work. Metrol. Ind. 4.0 IoT, 2019, pp. 323–328.
[190] D. Campolo, L. Schenato, L. Pi, X. Deng, E. Guglielmelli, Attitude estimation of a biologically inspired robotic housefly via multimodal sensor fusion, Adv. Robot. 23 (2009) 955–977.
[191] H. Chen, M.C. Schall, N.B. Fethke, Measuring upper arm elevation using an inertial measurement unit: An exploration of sensor fusion algorithms and gyroscope models, Appl. Ergon. 89 (2020), 103187.
[192] H. Chen, M.C. Schall, N. Fethke, Accuracy of angular displacements and velocities from inertial-based inclinometers, Appl. Ergon. 67 (2018) 151–161.
[193] J. Thienel, R.M. Sanner, A coupled nonlinear spacecraft attitude controller and observer with an unknown constant gyro bias and gyro noise, IEEE Trans. Automat. Contr. 48 (2003) 2011–2015.
[194] K. Masuya, T. Sugihara, M. Yamamoto, Design of complementary filter for high-fidelity attitude estimation based on sensor dynamics compensation with decoupled properties, Proc. IEEE Int. Conf. Robot. Autom. (2012) 606–611.
[195] L. Benziane, A. Benallegue, A.E. Hadri, A globally asymptotic attitude estimation using complementary filtering, in: 2012 IEEE Int. Conf. Robot. Biomimetics, ROBIO 2012, IEEE, 2012, pp. 878–883.
[196] M. Cheguini, F. Ruiz, Real-time attitude estimation based on Gradient Descent algorithm, in: 2012 IEEE 4th Colomb. Work. Circuits Syst., IEEE, Barranquilla, Colombia, 2012.
[197] M.S. Karunarathne, S.W. Ekanayake, P.N. Pathirana, An adaptive complementary filter for inertial sensor based data fusion to track upper body motion, in: 7th Int. Conf. Inf. Autom. Sustain. ICIAfS 2014, 2014.
[198] V. Kubelka, M. Reinstein, Complementary filtering approach to orientation estimation using inertial sensors only, in: Proc. IEEE Int. Conf. Robot. Autom., IEEE, 2012, pp. 599–605.
[199] M. Blachuta, R. Grygiel, R. Czyba, G. Szafranski, Attitude and heading reference system based on 3D complementary filter, in: 19th Int. Conf. Methods Model. Autom. Robot. MMAR 2014, IEEE, 2014, pp. 851–856.
[200] R.S. McGinnis, S.M. Cain, S.P. Davidson, R.V. Vitali, S.G. McLean, N.C. Perkins, Validation of complementary filter based IMU data fusion for tracking torso angle and rifle orientation, Int. Mech. Eng. Congr. Expo. (2014) 2014.
[201] X. Li, C. He, Y. Wang, Z. Li, Generalized complementary filter for attitude estimation based on vector observations and cross products, in: 2015 IEEE Int. Conf. Inf. Autom., IEEE, 2015, pp. 1733–1737.
[202] S.Q. Liu, R. Zhu, A complementary filter based on multi-sample rotation vector for attitude estimation, IEEE Sens. J. 18 (2018) 6686–6692.

[203] S. Wilson, H. Eberle, Y. Hayashi, S.O.H. Madgwick, A. Mcgregor, X. Jing, R. Vaidyanathan, Formulation of a new gradient descent MARG orientation algorithm: Case study on robot teleoperation, Mech. Syst. Signal Process. 130 (2019) 183–200.
[204] L. Wöhle, M. Gebhard, Steadeye-head—improving MARG-sensor based head orientation measurements through eye tracking data, Sensors (2020).
[205] M.L. Hoang, A. Pietrosanto, S. Dello Iacono, V. Paciello, Pre-processing technique for compass-less madgwick in heading estimation for industry 4.0, IEEE Int. Instrum. Meas. Technol. Conf. (2020).
[206] J.A. Barraza Madrigal, J. Cantillo Negrete, R. Muñoz Guerrero, L.A. Contreras Rodríguez, H. Sossa, 3D motion tracking of the shoulder joint with respect to the thorax using MARG sensors and data fusion algorithm, Biocybern. Biomed. Eng. 40 (2020) 1205–1224.
[207] J. Justa, V. Šmídl, A. Hamáček, Fast AHRS filter for accelerometer, magnetometer, and gyroscope combination with separated sensor corrections, Sensors (Switzerland) 20 (2020).
[208] Z. Peng, L. Guan, X. Xu, J. Zeng, Y. Gao, J. Yang, Real-time attitude estimation for high-speed UAV in high-frequency environmental dithering based on AMCF, in: China Satell. Navig. Conf. 2020, 2020, pp. 89–98.
[209] S.O.H. Madgwick, S. Wilson, R. Turk, J. Burridge, C. Kapatos, R. Vaidyanathan, An extended complementary filter for full-body MARG orientation estimation, IEEE/ASME Trans. Mechatronics. 25 (2020) 2054–2064.
[210] M. Haid, J. Breitenbach, Low cost inertial orientation tracking with Kalman filter, Appl. Math. Comput. 153 (2004) 567–575.
[211] J. Bijker, W. Steyn, Control engineering practice Kalman filter configurations for a low-cost loosely integrated inertial navigation system on an airship, Control Eng. Pract. 16 (2008) 1509–1518.
[212] P. Tome, O. Yalak, Improvement of orientation estimation in pedestrian navigation by compensation of magnetic disturbances, Navigation 55 (2008) 179–190.
[213] G. Cooper, I. Sheret, L. Mcmillian, K. Siliverdis, N. Sha, D. Hodgins, L. Kenney, D. Howard, Inertial sensor-based knee flexion/extension angle estimation, J. Biomech. 42 (2009) 2678–2685.
[214] C.M.N. Brigante, N. Abbate, A. Basile, A.C. Faulisi, S. Sessa, Towards miniaturization of a MEMS-based wearable motion capture system, IEEE Trans. Ind. Electron. 58 (2011) 3234–3241.
[215] A.R. Jiménez, F. Seco, J.C. Prieto, J. Guevara, Indoor pedestrian navigation using an INS/EKF framework for yaw drift reduction and a foot-mounted IMU, in: Proc. 7th Work. Positioning, Navig. Commun., 2010.
[216] J. Borestein, L. Ojeda, S. Kwanmuang, Heuristic reduction of gyro drift in IMU-based personnel tracking system, in: Procedding SPIE Defense, Secur. Sens. Conf., Orlando, Florida, USA, 2009.
[217] S. Sabatelli, F. Sechi, L. Fanucci, A. Rocchi, A sensor fusion algorithm for an integrated angular position estimation with inertial measurement units, in: Proceeding 2011 Des. Autom. Test Eur., 2011.
[218] S. Han, J. Wang, A novel method to integrate IMU and magnetometers in attitude and heading reference systems, J. Navig. 64 (2011) 727–738.
[219] R. Munguia, A. Grau, Attitude and heading system based on EKF total state configuration, in: Proceeding 2011 IEEE Int. Symp. Ind. Electron., IEEE, 2011, pp. 2147–2152.
[220] E. Edwan, J. Zhang, J. Zhou, O. Loffeld, Reduced DCM based attitude estimation using low-cost IMU and magnetometer triad, in: Proc. 2011 8th Work. Positioning, Navig. Commun., IEEE, 2011.
[221] M.H. Afzal, V. Renaudin, G. Lachapelle, Use of earth's magnetic field for mitigating gyroscope errors regardless of magnetic perturbation, Sensors 11 (2011) 11390–11414.
[222] J.K. Lee, E.J. Park, S.N. Robinovitch, Estimation of attitude and external acceleration using inertial sensor measurement during various dynamic conditions, IEEE Trans. Instrum. Meas. 61 (2012) 2262–2273.
[223] M. Carminati, G. Ferrari, R. Grassetti, M. Sampietro, Real-time data fusion and MEMS sensors fault detection in an aircraft emergency attitude unit based on kalman filtering, IEEE Sens. J. 12 (2012) 2984–2992.
[224] Z. Zhang, X. Meng, J. Wu, Quaternion-based kalman filter with vector selection for accurate orientation tracking, IEEE Trans. Instrum. Meas. 61 (2012) 2817–2824.
[225] W. Li, J. Wang, Effective adaptive kalman filter for MEMS-IMU/magnetometers integrated attitude and heading reference systems, J. Navig. 66 (2013) 99–113.
[226] Q. Zhang, X. Niu, H. Zhang, C. Shi, Algorithm improvement of the low-end GNSS/INS systems for land vehicles navigation, Hindawi Publ. Corp. Math. Probl. Eng. (2013).
[227] M. Jin, J. Zhao, J. Jin, G. Yu, W. Li, The adaptive Kalman filter based on fuzzy logic for inertial motion capture system, Measurement 49 (2014) 196–204.
[228] R. Munguía, A. Grau, A practical method for implementing an attitude and heading reference system, Int. J. Adv. Robot. Syst. 11 (2014).
[229] S. Zihajehzadeh, D. Loh, M. Lee, R. Hoskinson, E.J. Park, A cascaded two-step kalman filter for estimation of human body segment orientation using MEMS-IMU, in: Proc. 36th Annu. Int. Conf. IEEE Eng. Med. Biol. Soc., IEEE, 2014, pp. 6270–6273.
[230] C. Miao, Q. Zhang, J. Fang, Design of orientation estimation system by inertial and magnetic sensors, Proc. Inst. Mech. Eng. Part G J. Aerosp. Eng. 228 (2014) 1105–1113.
[231] Y. Wang, A. Hussain, M. Soltani, A MEMS-based adaptive AHRS for marine satellite tracking antenna, IFAC-PapersOnLine 48 (2015) 121–126.
[232] L. Wang, Z. Zhang, P. Sun, Quaternion-based kalman filter for AHRS using an adaptive-step gradient descent algorithm, Int. J. Adv. Robot. Syst. 12 (2015).
[233] Z. Deng, G. Wang, Y. Hu, D. Wu, Heading estimation for indoor pedestrian navigation using a smartphone in the pocket, Sensors 15 (2015) 21518–21536.
[234] P. Neto, N. Mendes, A.P. Moreira, Kalman filter-based yaw angle estimation by fusing inertial and magnetic sensing: a case study using low cost sensors, Sens. Rev. 35 (2015) 244–250.
[235] L.R. Lustosa, S. Pizziol, F. Defay, J.-M. Moschetta, An error model of a complementary filter for use in bayesian estimation - the CF-EKF filter, IFAC-PapersOnLine 49 (2016) 444–449.
[236] R.B. Widodo, C. Wada, Attitude estimation using kalman filtering: external acceleration compensation considerations, J. Sensors, Hindawi. (2016).
[237] C.W. Kang, H.J. Kim, C.G. Park, A human motion tracking algorithm using adaptive EKF based on markov chain, IEEE Sens. J. 16 (2016) 8953–8962.
[238] L. Chang, F. Zha, F. Qin, Indirect kalman filtering based attitude estimation for low-cost attitude and heading reference systems, IEEE/ASME Trans. Mechatronics. 22 (2017) 1850–1858.
[239] T. Zhang, Y. Liao, Attitude measure system based on extended Kalman filter for multi-rotors, Comput. Electron. Agric. 134 (2017) 19–26.
[240] P. Bernal-Polo, H. Martinez-Barbera, Orientation estimation by means of extended kalman filter, quaternions, and charts, J. Phys. Agents. 8 (2017) 11–24.
[241] Y. Wang, M. Soltani, D.M.A. Hussain, An attitude heading and reference system for marine satellite tracking antenna, IEEE Trans. Ind. Electron. 64 (2017) 3095–3104.
[242] S. Šlajpah, R. Kamnik, M. Munih, Compensation for magnetic disturbances in motion estimation to provide feedback to wearable robotic systems, IEEE Trans. Neural Syst. Rehabil. Eng. 25 (2017) 2398–2406.
[243] M.B. Del Rosario, H. Khamis, P. Ngo, N.H. Lovell, S.J. Redmond, Computationally efficient adaptive error-state kalman filter for attitude estimation, IEEE Sens. J. 18 (2018) 9332–9342.
[244] P.J. Glavine, O. De Silva, G. Mann, R. Gosine, P. Philip, S. John, N.L. Ab, GPS integrated inertial navigation system using interactive multiple model extended kalman filtering, in: Proc. 2018 Moratuwa Eng. Res. Conf., IEEE, 2018, pp. 414–419.
[245] Q. Yuan, E. Asadi, Q. Lu, G. Yang, I. Chen, Uncertainty-based IMU orientation tracking algorithm for dynamic motions, IEEE/ASME Trans. Mechatronics. 24 (2019) 872–882.
[246] H. Ahmed, I. Ullah, U. Khan, M.B. Qureshi, S. Manzoor, N. Muhammad, M.U. S. Khan, R. Nawaz, Adaptive filtering on gps-aided mems-imu for optimal estimation of ground vehicle trajectory, Sensors (Switzerland) 19 (2019) 1–18.
[247] A.P. Sage, G.W. Husa, Adaptive filtering with unknown prior statistics, IEEE Trans. Autom. Control. 7 (1969) 760–769.
[248] Q. Ge, T. Shao, C. Wen, R. Sun, Analysis on strong tracking filtering for linear dynamic systems, Math. Probl. Eng. 2015 (2015).
[249] H.T. Butt, M. Pancholi, M. Musahl, P. Murthy, M.A. Sanchez, D. Stricker, Inertial motion capture using adaptive sensor fusion and joint angle drift correction, in: 22nd Int. Conf. Inf. Fusion, 2019.
[250] Q. Fan, H. Zhang, P. Pan, X. Zhuang, J. Jia, P. Zhang, Z. Zhao, G. Zhu, Y. Tang, Improved pedestrian dead reckoning based on a robust adaptive Kalman filter for indoor inertial location system, Sensors (Switzerland) 19 (2019).
[251] Á. Odry, I. Kecskes, P. Sarcevic, Z. Vizvari, A. Toth, P. Odry, A novel fuzzy-adaptive extended kalman filter for real-time attitude estimation of mobile robots, Sensors (2020).
[252] K. Wen, K. Yu, Y. Li, S. Zhang, W. Zhang, A new quaternion kalman filter based foot-mounted IMU and UWB tightly-coupled method for indoor pedestrian navigation, IEEE Trans. Veh. Technol. 69 (2020) 4340–4352.
[253] M.A. Javed, M. Tahir, K. Ali, Cascaded kalman filtering-based attitude and gyro bias estimation with efficient compensation of external accelerations, IEEE Access 8 (2020) 50022–50035.
[254] M. Ji, J. Liu, X. Xu, Y. Guo, Z. Lu, Improved pedestrian positioning with inertial sensor based on adaptive gradient descent and double-constrained extended kalman filter, Complexity, Hindawi (2020).
[255] F. Farhangian, R. Landry Jr., Accuracy improvement of attitude determination systems using EKF-based error prediction filter and PI controller, Sensors (Switzerland) 20 (2020) 4055.
[256] H. Du, W. Wang, C. Xu, R. Xiao, C. Sun, Real-time onboard 3D state estimation of an unmanned aerial vehicle in multi-environments using multi-sensor data fusion, Sensors (Switzerland) 20 (2020).
[257] S. Park, J. Park, C.G. Park, Adaptive attitude estimation for low-cost MEMS IMU using ellipsoidal method, IEEE Trans. Instrum. Meas. 69 (2020) 7082–7091.